Unit descriptions for bedrock geologic maps of the Chena-Pogo map area, Alaska

Rainer J. Newberry Evan Twelker, Travis J. Naibert, Michael L. Barrera, David J. Szumigala, J. Wesley Buchanan, Conner M. Truskowski, Kelly R. Wilson

PIR 2026-3A

Interlayered granitic and mafic gneiss of the Lake George assemblage, field station 24JWB067. Photo taken June 26, 2024, by J.W. Buchanan.

Preliminary Interpretive Reports present emergent interpretations of geologic mapping or analytical investigation. These publications are reviewed for clarity and consistency and receive limited peer review.

State of Alaska
Department of Natural Resource
Division of Geological & Geophysical Surveys

State of Alaska
Mike Dunleavy, Governor

Department of Natural Resources
John Crowther, Commissioner

Division of Geological & Geophysical Surveys
Erin A. Campbell, State Geologist & Director

Publications produced by the Division of Geological & Geophysical Surveys are available to download from the DGGS website (http://dggs.alaska.gov/). Publications on hard-copy or digital media can be examined or purchased in the Fairbanks office:

Alaska Division of Geological & Geophysical Surveys (DGGS)
3354 College Road | Fairbanks, Alaska 99709-3707
Phone: 907.451.5010 | Fax 907.451.5050
dggspubs@alaska.gov | dggs.alaska.gov

DGGS publications are also available at:
Alaska State Library, Historical
Collections & Talking Book Center
395 Whittier Street
Juneau, Alaska 99801

Alaska Resource Library and
Information Services (ARLIS)
3150 C Street, Suite 100
Anchorage, Alaska 99503

Suggested citation:
Newberry, R.J., Twelker, Evan, Naibert, T.J., Barrera, M.L., Szumigala, D.J., Buchanan, J.W., Truskowski, C.M., and Wilson, K.R., 2026, Unit descriptions for bedrock geologic maps of the Chena-Pogo map area, Alaska, in Twelker, Evan, ed., Geologic investigation of the Chena-Pogo area, interior Alaska: Alaska Division of Geological & Geophysical Surveys Preliminary Interpretive Report 2026-3A, 63 p. https://doi.org/10.14509/32112

Unit descriptions for bedrock geologic maps of the Chena-Pogo map area, Alaska

Rainer J. Newberry[1], Evan Twelker[1], Travis J. Naibert[1], Michael L. Barrera[1], David J. Szumigala[1], J. Wesley Buchanan[1], Conner M. Truskowski[1], Kelly R. Wilson[1]

ABSTRACT

The Chena-Pogo project updates the bedrock geologic mapping of a 14,530-sq-km (5,610-sq-mi) area in the Yukon-Tanana Upland (YTU) of eastern Interior Alaska. The goals of the project are to better understand the geologic framework of known mineralization, to support the exploration and discovery of new mineral resources in the area, and to build scientific understanding of the geology of the YTU, one of Alaska's most active and important mineral belts. The project area has been a focus of gold exploration for several decades but also has additional significance for its potential to host critical minerals such as antimony, bismuth, tellurium, and tungsten.

Project work was completed by Alaska Division of Geological & Geophysical Surveys (DGGS) staff and collaborators during 2023, 2024, and 2025 field seasons and draws on additional published and unpublished work completed during prior years by DGGS, University of Alaska, and U.S. Geological Survey staff.

The Chena-Pogo project is divided into four 1:100,000-scale map sheets NW Chena, NE Chena, SW Chena, and SE Chena (fig. 1). The map units used across the four maps are described in this report. For geographic information system (GIS) users, the four maps are distributed as a single geologic map database using either the standard Geologic Mapping Schema (GeMS) or the Alaska Geologic Mapping Schema (AK GeMS; Hendricks and others, 2024). U-Pb zircon ages generated as part of this project and referenced in this report are compiled in Table A–1. A statistical summary of magnetic susceptibility by map unit is provided in Table A–2. All publication components are available from the DGGS website at https://doi.org/10.14509/32111.

METHODS

The Alaska Division of Geological & Geophysical Surveys (DGGS) Mineral Resources Section conducted bedrock geologic mapping of the 14,530 sq-km (5,610 sq-mi) Chena-Pogo project in the Yukon-Tanana Upland (YTU) of Interior Alaska during the 2023, 2024, and 2025 field seasons. Staff collected 4,800 bedrock stations, 429 geochemical samples, and 51 geochronology samples. Parts of the project area already mapped in detail by DGGS and the U.S. Geological Survey (USGS) have been compiled into this project, including maps of the Salcha River-Pogo area (Werdon and others, 2004), the Big Delta B-2 and B-1 quadrangles (Day and others, 2003; Day and others, 2007), Caribou Creek (Lessard, 2006), Nail Ridge (Southworth, 1984), and the Upper Chena River (Smith and others, 1994). These prior maps have been

[1] Alaska Division of Geological & Geophysical Surveys, 3354 College Road, Fairbanks, AK 99709

modified to 1) match original map units to the units of this publication; 2) remove surficial geology, if present; 3) simplify geology as necessary for display at 1:100,000 scale; and 4) change interpretations based on new information.

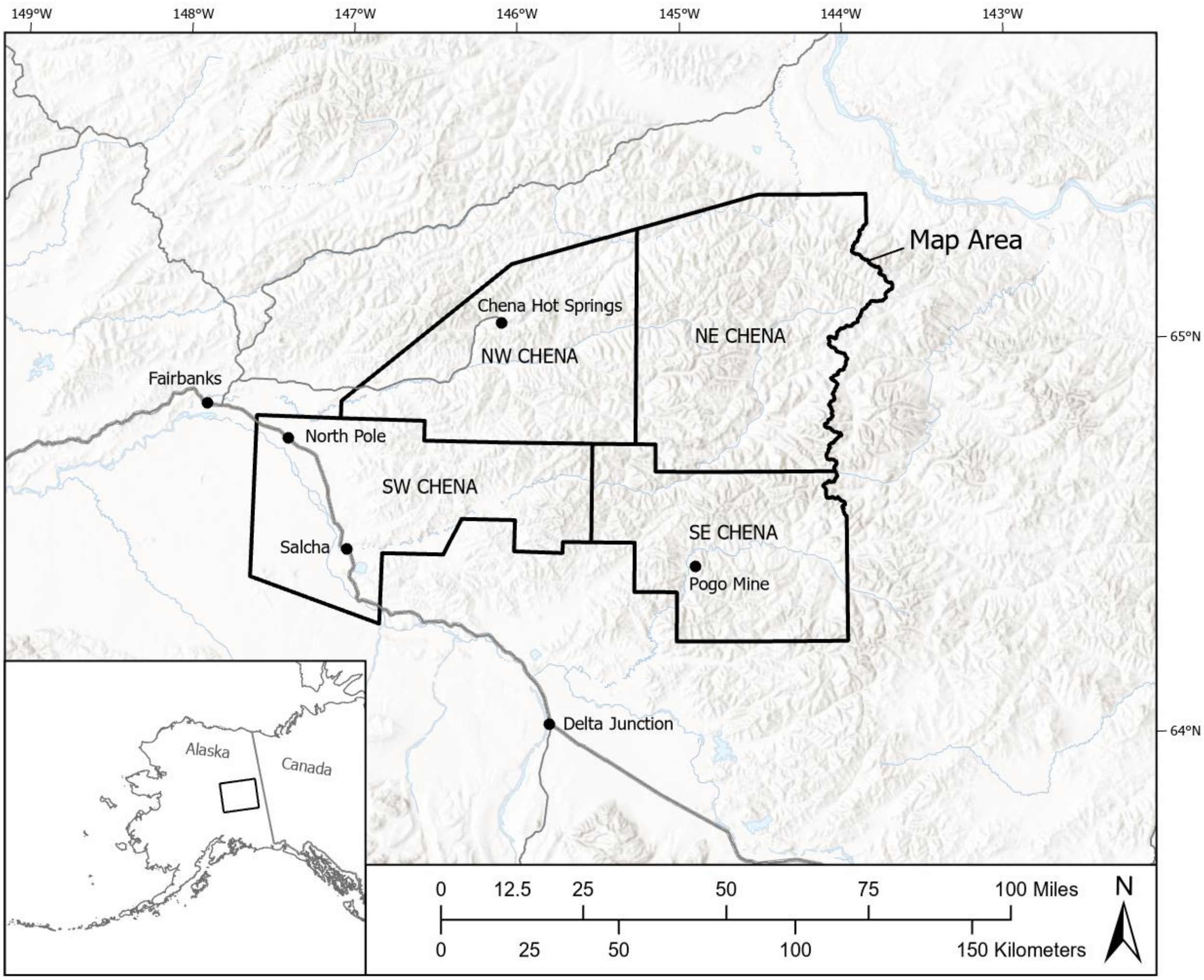

Figure 1. Geographic location of the project area and the four associated map sheets.

DESCRIPTION OF MAP UNITS

Sedimentary Rocks

CzKs SEDIMENTARY ROCKS, UNDIVIDED (CRETACEOUS TO CENOZOIC)—Sandstone, conglomerate, and local shale. Sandstone is typically coarse-grained, poorly sorted, clast-supported, and well indurated, with abundant feldspar and lithic fragments. Conglomerate is compositionally similar and contains poorly sorted, subrounded to rounded clasts, including a significant feldspar component. Shale is present locally. In the upper Goodpaster River area of the SE Chena map, the unit is overlain by Paleogene rhyolite (unit Pɛr). Magnetic susceptibility is low, ranging from 0.007–0.1 x 10^{-3} Système International (SI), with an average and median of 0.04 x 10^{-3} SI. The maximum depositional age is constrained by a detrital zircon population at 69 Ma (sample 23AW034; unit CzKs; Buchanan, Barrera, Gavel and others, 2026)

Igneous Rocks

Volcanic Rocks

Pɛr RHYOLITE (PALEOGENE)—Rhyolite, including tuff, rocks of possible hypabyssal origin, and local mafic dikes. Lithic crystal tuff contains 30 percent crystals, including quartz, alkali feldspar, plagioclase, biotite and hornblende, and 20 percent lithic fragments, including granitic clasts up to 5 mm. Rhyolitic rocks lacking macroscopic volcaniclastic textures locally display columnar jointing and spherulites. Based on a single station, the magnetic susceptibility can be elevated (3.8–6.0 x 10^{-3} SI), with an average of 4.7 x 10^{-3} and a median of 4.6 x 10^{-3} SI. Age is constrained by U-Pb zircon ages of 57.15 ± 1.6 Ma (sample 19ADK047; Holm-Denoma and others, 2022) and 57.2 ± 0.6 Ma (sample 04AD239; Day and others, 2007). Age, bulk composition, and proximity strongly suggest this unit is the extrusive equivalent of felsic porphyry in the Slate Creek intrusive suite (Pɛfp).

Plutonic Rocks

Slate Creek Intrusive Suite

The Slate Creek intrusive suite (informal; Twelker and others, 2025; this study) comprises volumetrically minor, bimodal mafic and felsic igneous rocks mapped in the western Yukon-Tanana Upland. The suite is named for the Slate Creek pluton in the northeastern quadrant of the SE Chena map.

Pɛfp FELSIC PORPHYRY (PALEOGENE)—Small stocks of granite, porphyritic granite, and granite porphyry, as well as scattered dikes with similar textures. Locally includes granodiorite porphyry, quartz monzonite, and equigranular rocks. Felsic rocks invariably plot as 'within-plate granite' based on trace-element content (Buchanan, Wypych, and others, 2025). Phenocrysts include quartz, alkali feldspar, plagioclase, and biotite; other primary minerals locally present include garnet, white mica, and rare topaz. Secondary minerals include sericite, chlorite, rutile, and local tourmaline.

Groundmass grain size is 20–100 μm (0.02–0.1 mm) in porphyritic samples, and up to 0.4 mm in semi-equigranular samples. Magnetic susceptibility is low, 0.01–0.86 x 10^{-3} SI, with an average of 0.2 x 10^{-3} SI and a median of 0.09 x 10^{-3} SI. U-Pb zircon crystallization ages include 57.89 ± 0.46 Ma (sample 23ET064), 59.86 ± 0.26 Ma (sample 23ET223), and 57.32 ± 0.37 Ma (sample 23TJN040; Buchanan, Gavel, Barrera, and others, 2025). We interpret this unit to represent the felsic component of a bimodal igneous suite associated with crustal extension.

₽m MAFIC INTRUSIONS (PALEOGENE)—Rare, volumetrically minor dikes or small stocks of gabbro to diorite, typically with significant hydrothermal alteration. Textures are fine-grained and porphyritic to seriate. Primary mineralogy includes plagioclase, biotite, hornblende, augite, and lesser orthopyroxene, alkali feldspar, apatite, ilmenite, and magnetite. Secondary minerals include minor to major chlorite, calcite, quartz, and sericite. Magnetic susceptibility is mostly moderate, 0.15–3.2 x 10^{-3} SI, with a median value of 0.74 x 10^{-3} SI. Age of emplacement is constrained by U-Pb zircon ages of 56.6 ± 0.4 Ma (sample 22TJN285; Buchanan, Gavel, Wildland, and others, 2025) and 56.71 ± 0.37 Ma (sample 23ADW001; Buchanan, Gavel, Barrera, and others, 2025). Trace-element geochemistry is consistent with a within-plate tectonic setting (diagrams of Pearce and Cann, 1973; Meschede, 1986). We interpret this unit as the intrusive equivalent of ca. 55 Ma basalts, such as the Browns Hill Quarry basalt (unit Tb) of Newberry and others (1996).

Eielson Plutonic Suite

The herein-named Eielson plutonic suite consists of latest-Cretaceous granitic rocks in the western Yukon-Tanana Upland, and is named for the Eielson pluton near Salcha, Alaska (center-left, SW Chena map). It is distinguished from the Taurus plutonic suite by its geographic distribution and by its characteristically lower magnetic susceptibility.

lKeg GRANITE (LATEST CRETACEOUS)—Pluton- and stock-sized bodies of granite, mostly present in the western part of the Chena-Pogo project area, but also on a ridge along the axis of an antiform north of the upper Chena River (Smith and others, 1994). Granite is dominantly medium-grained and porphyritic, with alkali feldspar phenocrysts 5- to 20-mm long and includes seriate and sub-equigranular textural variants. Granite porphyry is restricted to the northernmost part of the Eielson pluton (SW Chena map). Sheared granite is locally present in the north-central part of the Chena Hot Springs batholith (NW Chena map). Eielson suite granite is most reliably distinguished from Fairbanks-Salcha suite granite based on U-Pb ages and generally higher Nb+Y for the former (Buchanan, Wypych, and others, 2025; Moshrefzadeh and others, 2025). Primary minerals include quartz, alkali feldspar, plagioclase, biotite, and ilmenite. The alkali feldspar granite at Moose Creek Bluff also contains ferro-edenite amphibole. White mica locally appears to be primary, but texturally secondary white mica is nearly ubiquitous. Secondary chlorite after biotite is common. Secondary tourmaline occurs in the Eielson pluton and locally in other Eielson suite granites. Granite of the Eielson suite has a mostly low magnetic susceptibility (0.01–3.0 x 10^{-3} SI, with an average of 0.14 x 10^{-3} SI and a median of 0.06 x 10^{-3} SI). The age of crystallization is constrained by 12 U-Pb zircon ages between 66 and 77 Ma (samples 23TJN064, 24CMT102, 23JWB145, 24Z312, 23Z388, 23Z467, 24MLB181, 23RN276, 24Z315; Buchanan, Barrera, and others, 2025; samples 23IPM132, 23MLB206, 23RN540; Buchanan, Gavel, Barerra, and others, 2025).

Taurus Plutonic Suite

The Taurus plutonic suite (Wypych and others, 2021; Naibert and others, 2024) comprises felsic to intermediate granitic rocks that are mapped mostly in the eastern Yukon-Tanana Upland; only isolated occurrences of this unit are mapped in the SE Chena and NE Chena map sheets.

lKpg

PORPHYRITIC GRANITE (LATEST CRETACEOUS?)—Porphyritic granite is mapped in upper Paldo Creek (southeastern NE Chena map). It is characterized by phenocrysts of alkali feldspar (megacrystic, 25 to 70 mm), plagioclase, quartz, and biotite in a fine-grained holocrystalline groundmass. Minor primary(?) phases include magnetite, ilmenite, epidote, titanite, and allanite. Secondary minerals include minor sericite, chlorite, and epidote. The Paldo Creek intrusion shows up as a distinctive magnetic high (Emond and MPX Geophysics, Ltd., 2022) and is characterized by elevated magnetic susceptibility (0.03–6 x 10^{-3} SI, average of 1.2 x 10^{-3} SI and median of 0.65 x 10^{-3} SI). Low values are from highly altered and mineralized samples and are not representative of the body as a whole. In the Camp Creek area (Big Delta C-3 Quadrangle), Werdon and others (2004) describe hypabyssal stocks and dikes of altered granite and granodiorite (their unit Khg) within the Butte assemblage, dated at approximately 69 Ma by ^{40}Ar/^{39}Ar on biotite. Additionally, a sample of monzogranite, associated with an aeromagnetic high 5 km east of the Paldo Creek intrusion, yielded a U-Pb zircon age of 79.6 ± 0.87 Ma (sample 19ADK074; Kreiner and others, 2025). This unit is correlated with the Taurus plutonic suite to the east and south of the Shaw Creek Fault (Twelker and others, 2025). Though their Late Cretaceous ages overlap, Taurus plutonic suite intrusions have markedly higher magnetic susceptibility than intrusions of the Eielson plutonic suite described above.

Fairbanks-Salcha Plutonic Suite

The Fairbanks-Salcha plutonic suite includes calc-alkaline granitic rocks and lesser mafic to intermediate intrusive rocks emplaced ca. 90–99 Ma. Intrusions of this suite are typically stocks and plutons but also appear in composite batholiths with Eielson and Slate Creek suite rocks; they are distinctly younger than the batholith-forming Harper plutonic suite (described below). The Fairbanks-Salcha plutonic suite differs from the Gardiner plutonic suite by its geographic center in the Fairbanks and Salcha River areas and typically has a lower magnetic susceptibility (Twelker and others, 2025). The name for this suite follows Hart and others (2004).

Kfsg

GRANITE OF FAIRBANKS-SALCHA SUITE (EARLY LATE CRETACEOUS)—Pluton-and stock-sized bodies of granite, as well as lesser granodiorite and tonalite, occur throughout the map area, but form a batholith-scale intrusion in the Chena Hot Springs area (NW Chena map). The dominant textural variant is medium-grained and porphyritic, with alkali feldspar phenocrysts 10- to 20-mm long; fine- and medium-grained equigranular variants are also included in this unit. Primary minerals include quartz, alkali feldspar, plagioclase, biotite, hornblende (minor, locally present), and ilmenite. Primary white mica and local garnet are present in a minority of samples. Secondary minerals include chlorite, white mica, and calcite. Granite of the Fairbanks-Salcha suite is notable for its low magnetic susceptibility: 0.01–0.63 x 10^{-3} SI, with an average of 0.11 x 10^{-3} SI and a median of 0.09 x 10^{-3} SI. Age of crystallization is constrained by multiple U-Pb zircon ages ranging from 90–96 Ma (samples 23JNB024, 24JWB095, 24RN358, 23RN618, 23Z331; Buchanan, Barrera, and others, 2025; samples 23RN166, 23RN386, 23IPM200, 23Z330, 23RN248, 23Z150; Buchanan, Gavel, Barerra, and others, 2025).

Kfsgd

GRANODIORITE OF FAIRBANKS-SALCHA SUITE (EARLY LATE CRETACEOUS)—Small plutons or stocks of seriate, fine-grained granodiorite, and lesser granite, tonalite, and quartz diorite mapped across the project area, including as part of composite batholiths at Chena Hot Springs and Granite Tors (NW Chena map). Primary mineralogy includes plagioclase, alkali feldspar, quartz, biotite (1–30 percent), and hornblende (1–20 percent); secondary minerals include variable chlorite and sericite. Magnetic susceptibility is low but slightly higher than Fairbanks-Salcha suite granite (unit Kfsg): 0.02–8.5 x 10^{-3} SI, with an average of 0.34 x 10^{-3} SI and a median of 0.14 x 10^{-3} SI. U-Pb zircon crystallization ages range from 90 to 98 Ma (Buchanan, Barrera, and others, 2025; Buchanan, Gavel, Wildland, and others, 2025).

Kfsp

PORPHYRY OF FAIRBANKS-SALCHA SUITE (EARLY LATE CRETACEOUS)—Dike- to stock-sized bodies of fine-grained, porphyritic rocks with granite to granodiorite compositions. Phenocrysts, generally less than 10 mm, include quartz, alkali feldspar, plagioclase, biotite, and local hornblende; groundmass grain size is 0.05–0.2 mm (50–200 µm). Secondary minerals include variably abundant chlorite, sericite, and pyrite. Magnetic susceptibility is generally low but variable: 0.00–1.8 x 10^{-3} SI, with an average of 0.4 x 10^{-3} SI and a median of 0.07 x 10^{-3} SI. Crystallization age is constrained by U-Pb zircon ages of 94.99 ± 0.77 Ma (laser ablation-inductively coupled plasma-mass spectrometry [LA-ICP-MS]; Kreiner and others, 2025; sample

22ADK046a) and 99.5 ± 0.9 Ma (sensitive high-mass-resolution mass spectrometry [SHRIMP]; sample 05AD353; Day and others, 2007).

Kfsqd QUARTZ DIORITE OF FAIRBANKS-SALCHA SUITE (EARLY LATE CRETACEOUS)—Small stocks of quartz monzodiorite, quartz diorite, tonalite, and diorite. They are mapped mostly in the Goodpaster River-Pogo mine area (SE Chena map), but also locally in the Granite Tors area (NW Chena map). These intrusions are typically fine-grained, seriate to equigranular, and locally porphyritic. Primary minerals include plagioclase, alkali feldspar, quartz, biotite (10–15 percent), augite, and lesser orthopyroxene (0.5–20 percent), hornblende (5–10 percent; rimming pyroxenes), apatite, ilmenite, and local magnetite. Locally present secondary minerals include actinolite, chlorite, and calcite; titanite is likely secondary. Magnetic susceptibility is the highest of this suite: 0.07–7.4 x 10^{-3} SI, with an average of 0.62 x 10^{-3} SI and a median of 0.26 x 10^{-3} SI. U-Pb zircon crystallization ages range from 93 to 101 Ma (sample 24ET154; Buchanan, Barrera and others, 2025; sample 23RN183; Buchanan, Gavel, Barerra, and others, 2025); Kreiner and others (2025) obtained LA-ICP-MS zircon ages ranging from 93–97 Ma from eight samples of different compositional phases of this unit collected at the Pogo mine. Unit includes tonalite (unit Ktn) of Werdon and others (2004), diorite and tonalite (unit Kdt) of Day and others (2003), and the Liese Creek diorite of Smith and others (1999).

Kfsmg WHITE MICA-BEARING GRANITE OF FAIRBANKS-SALCHA SUITE (EARLY LATE CRETACEOUS)—Fine- to medium-grained, seriate to equigranular, muscovite- and/or garnet-bearing peraluminous granite. Occurs as a phase of the Chena Hot Springs (NW Chena map) and Thanksgiving Creek batholiths (NE Chena map). Primary mineralogy includes alkali feldspar, quartz, plagioclase, biotite (2–4 percent), muscovite (1–4 percent), and garnet (0–1 percent); locally developed secondary minerals include chlorite (after biotite), sericite, calcite, and epidote. Magnetic susceptibility is uniformly low: 0.01–0.76 x 10^{-3} SI, with an average of 0.09 x 10^{-3} SI and a median of 0.06 x 10^{-3} SI. Age of crystallization is constrained by a U-Pb zircon age of 97.4 ± 0.78 Ma (sample 23RN487; Buchanan, Gavel, Barrera, and others, 2025). Distinguished from unit Khmg chiefly by its younger age of crystallization.

Kfst TONALITE OF FAIRBANKS-SALCHA SUITE (EARLY LATE CRETACEOUS)—Small stocks or plutons of tonalite and locally quartz diorite; fine-grained equigranular, seriate, or porphyritic. Primary mineralogy includes plagioclase, quartz, alkali feldspar, biotite (12–17 percent), hornblende (4–13 percent), and, in some samples, augite (partially replaced by hornblende). Variable secondary alteration minerals include chlorite, sericite, titanite, clinozoisite, and calcite. Magnetic susceptibility ranges from 0.1–0.7 × 10^{-3} SI, with an average of 0.24 × 10^{-3} SI and a median of 0.25 × 10^{-3} SI. Age of crystallization is constrained by a U-Pb zircon age of 96.5 ± 0.49 Ma (sample 24MLB029; Buchanan, Barrera, and others, 2025).

Harper Plutonic Suite

The Harper plutonic suite comprises calc-alkaline granitic rocks, plus minor mafic and intermediate intrusive rocks, emplaced in the central YTU ca. 105–112 Ma. It is named for its largest constituent body, the Mount Harper batholith (Day and others, 2007; Gavel and others, 2025) and includes the Goodpaster batholith.

Khg

GRANITE OF HARPER SUITE (LATE EARLY CRETACEOUS)—Stocks and plutons of granite, plus lesser granodiorite and other granitic rocks, the bulk of which form composite batholiths with other Harper suite units. The rocks are typically fine to medium and locally coarse-grained, equigranular to seriate, and locally porphyritic. Primary mineralogy includes quartz, alkali feldspar, plagioclase, and biotite (1–10 percent). Muscovite, magnetite, garnet, and hornblende occur as primary minerals in a minority of samples. Secondary minerals include chlorite, epidote, sericite, and calcite, which partially replace primary phases. The Harper plutonic suite is characterized by a broad range of magnetic susceptibility that does not vary much with degree of fractionation; this unit ranges from 0.01 to 3.7 x 10^{-3} SI, with an average of 0.22 x 10^{-3} SI and a median of 0.11 x 10^{-3} SI. Age of crystallization is constrained by multiple U-Pb zircon ages ca. 106–111 Ma (sample 24Z054; Buchanan, Barrera, and others, 2025; sample 23MMG150, 23IPM068; Buchanan, Gavel, Barerra, and others, 2025).

Khgd

GRANODIORITE OF HARPER SUITE (LATE EARLY CRETACEOUS)—The major phase in the Goodpaster and Mount Harper batholiths, plus smaller bodies in the vicinity (SE Chena map). Granodiorite and up to 20 percent granite are the most abundant lithologies, with minor tonalite and rare quartz diorite. Typically, fine to medium grained and seriate, but locally porphyritic. Primary minerals in the granodiorite phase include plagioclase, quartz, alkali feldspar, biotite (5–15 percent), hornblende (2–6 percent), trace allanite, and in many samples, trace magnetite and/or ilmenite. Secondary minerals include chlorite (variably replacing biotite and hornblende), sericite (variably replacing plagioclase cores), titanite, epidote, and local calcite. Magnetic susceptibility is somewhat higher (0.02–12.3 x 10^{-3} SI, with an average of 0.53 x 10^{-3} SI and a median of 0.13 x 10^{-3} SI) than Harper granite (unit Khg). Age of crystallization is constrained by multiple U-Pb zircon ages ca. 106–112 Ma.

Unit includes unit Kgcd of Day and others (2003, 2007), which they describe as granitic dikes and plugs (mostly fine-grained granodiorite, lesser granite and pegmatite) mapped to the south of the Goodpaster Batholith (SE Chena map).

Khmg

MUSCOVITE-BEARING GRANITE OF HARPER SUITE (LATE EARLY CRETACEOUS)—As described by Werdon and others (2004), this unit comprises "fine- to coarse-grained, leucocratic, equigranular, generally non-foliated, but locally, moderately foliated granite… Occurs as a 10-km-long, northwest-trending, elongate intrusion in the west-central Big Delta C-3 Quadrangle (SE Chena map) surrounded by hundreds of small tourmaline–muscovite–garnet granite dikes, sills, and small plutons…Texturally varies from aplite to pegmatite, with consistently peraluminous granite major-oxide and modal composition… Average modal composition approximately 40 percent quartz, 30 percent K-feldspar, 15 percent plagioclase, 5–10 percent biotite, 3–12 percent muscovite, 0–2 percent garnet, 0–5 percent tourmaline, and 1 percent accessory minerals, including zircon, apatite, and ilmenite. Proportions of muscovite, biotite, garnet, and tourmaline vary widely. Magnetic susceptibility is very low ($0.00–0.17 \times 10^{-3}$ SI, average 0.05×10^{-3} SI)." DGGS did not revisit this unit during the 2023–2024 fieldwork.

Geochronology results from this unit include a $^{40}Ar/^{39}Ar$ muscovite plateau age of 108.2 ± 0.9 Ma (Werdon and others, 2004) and a U-Pb monazite age of 107.9 ± 1.2 Ma (Dilworth, 2003), which we interpret as the minimum crystallization ages. These ages make unit Khmg broadly coeval with other units of the Harper plutonic suite and distinguish it from the younger (ca. 97 Ma) and compositionally similar muscovite-bearing granites of the Fairbanks-Salcha suite (unit Kfsmg).

Khdi

DIORITE OF HARPER SUITE (LATE EARLY CRETACEOUS)—As described by Day and others (2007), this unit (in SE Chena map) comprises "dark-gray to dark-green, non-foliated biotite-hornblende diorite dikes. Unit contains distinctive medium-grained, subhedral hornblende-biotite and plagioclase phenocrysts and glomerocrysts set in a fine-grained dioritic matrix; interpreted to be emplaced as subvolcanic dikes and small intrusions." Unit is "emplaced as northeast-trending dikes within and along Black Mountain tectonic zone; displays aphanitic, chilled margin where it cuts unit Kbm" (Day and others, 2007; Kbm is compiled as unit Khg of this publication). The crystallization age is constrained by U-Pb zircon ages of 107.9 ± 1.1 Ma and 109.0 ± 1.1 Ma (SHRIMP; Day and others, 2007). DGGS did not revisit this unit during the 2023–2024 fieldwork.

Kmi

MAFIC TO INTERMEDIATE DIKES (MID-CRETACEOUS)—Dikes and volumetrically minor mafic intrusions of gabbro, diorite, and quartz diorite. Mapped mostly south and west of the Pogo mine (SE Chena map). Dikes are holocrystalline, fine-grained, and range from equigranular to porphyritic. Primary mineralogy is dominated by hornblende and plagioclase, with clinopyroxene in some samples, and minor biotite, quartz, and titanite. Alteration is variable, including chlorite, clinozoisite, sericite, and calcite. Emplacement of this unit is loosely constrained as postmetamorphic (Early to mid-Cretaceous), but its chemical composition (Werdon and others, 2001; Athey and others, 2002; Werdon and others, 2003) differs from that of Paleogene gabbros (unit Pɛm). A sample of this unit (23IPM033) yielded a ^{40}Ar/^{39}Ar isochron age of 104.76 ± 2.05 Ma (Moshrefzadeh and others, 2026).

KPzi INJECTION MIGMATITE (CRETACEOUS TO PALEOZOIC) — As described by Werdon and others (2004), "Migmatite formed by the injection of numerous small (centimeter-scale) granite sills and dikes with diffuse boundaries…into hornfelsed paragneiss… Noticeably a mixed rock, even at a hand-specimen scale. Granite sills and dikes possess variable textures, but are most commonly medium-grained, equigranular. Modal abundances average 30–40 percent quartz, 20–30 percent plagioclase, 30–40 percent K-feldspar, and 5–10 percent combined biotite and muscovite. The hornfelsed paragneiss portions invariably contain rounded clots, 3–7 cm in diameter, of coarse-grained, partly retrograded cordierite and fine-grained, randomly oriented biotite. On average, the hornfelsed paragneiss portions contain 10–25 percent cordierite (now largely retrograded to fine-grained pinite), 3–8 percent sillimanite as randomly oriented grains in biotite, 1–3 percent garnet, 40–60 percent quartz, and 10–30 percent feldspar with K-feldspar > plagioclase. Forms massive, bold outcrops and subcrops invariably covered with orange-brown iron-oxide staining. Only freshly broken, and especially large, sawed slabs are confidently identified as the injection migmatite due to the extensive weathering surfaces and small granite sills and dikes. Magnetic susceptibility ranges from 0.05–0.35 x 10^{-3} and averages 0.12 x 10^{-3} SI."

Metamorphic Rocks

Oceanic Affinity Rocks of the Seventymile Terrane

Serpentinized ultramafic rocks, together with metamafic and metasedimentary rocks of the Seventymile Terrane, occur together in the southern part of the NE Chena map. The Seventymile Terrane is interpreted to represent a dismembered ophiolite (Foster and others, 1994; Werdon and others, 2004). Metamafic rocks yield mid-ocean ridge (MORB) trace-element signatures (Werdon and others, 2004; Buchanan, Wypych, and others, 2025). These rocks have been metamorphosed to prehnite-pumpellyite and greenschist facies. Following Werdon and others (2004), we recognize two different types of metasedimentary rocks, mostly present with fine-grained metamafic rocks: metachert and metaclastic rocks. The Seventymile assemblage displays an apparent inverted structural stacking, with serpentinized ultramafic rocks mostly at the highest structural level, resting on the other Seventymile subunits, or on Butte assemblage rocks (described below). However, metagabbroic rocks are locally mapped overlying meta-ultramafic rocks (Southworth, 1984), suggesting thrust imbrication.

Age constraints are both fossil and radiometric. Radiolaria and conodonts from metachert in the map area yield late Pennsylvanian to early Permian ages (Dusel-Bacon and Harris, 2003). Metalimestone and metachert from 140 km east of the map area yield late Triassic conodonts and Mississippian radiolaria, respectively (Dusel-Bacon and Harris, 2003). Hornblende from gabbro in the study area yielded Mississippian $^{40}Ar/^{39}Ar$ plateau and pseudo-plateau ages (Werdon and others, 2004). Todd and others (2023) present latest Permian to late Triassic U-Pb crystallization ages for metamafic bodies with ambiguous field relationships, either within or on top of the meta-ultramafic rocks in the map area. Given these constraints, we view the entire assemblage as Triassic to Mississippian.

Following Weber and others (1978), we view the entire Seventymile assemblage as thrust over the Butte assemblage rocks in the map area, with meta-ultramafic rocks mostly thrust over the other Seventymile subunits. Metamafic rocks are shown as interlayered with mixed metamafic/metasedimentary units, but intra-unit low-angle faults cannot be ruled out. Emplacement of the Seventymile terrane above the Butte assemblage is pre-Early Cretaceous, as plutons of that age are undeformed in the Chena map area, but could be as old as early Jurassic (Dusel-Bacon and others, 2002).

ꞦMsmm

METAMAFIC ROCKS OF THE SEVENTYMILE TERRANE (TRIASSIC TO MISSISSIPPIAN)—A texturally variable, but compositionally uniform, unit that accounts for nearly half of the Seventymile Terrane in the map area. Based on 42 analyses of samples collected between 2002 and 2024 (Werdon and others, 2003; Buchanan, Wypych, and others, 2025; Moshrefzadeh and others, 2025), these rocks possess 44–54 percent SiO_2 (basalt-basaltic andesite) with relatively low concentrations of TiO_2 (0.5–1.6 percent), P_2O_5 (0.05–0.22 percent), and Nb (0.2–6 parts per million). The low Nb is especially distinctive and serves to distinguish these from locally similar-appearing metamafic rocks of the Butte assemblage. Metamafic rocks most commonly appear as small (0.8 sq km) to medium (24 sq km) bodies that mostly sit structurally below Seventymile ultramafic rocks and above Butte assemblage rocks. Very small (<0.1 sq km) bodies also occur with ultramafic bodies in ambiguous relations. Southworth (1984) described them as occurring on top of ultramafic rocks; dikes in ultramafic rocks are also reported (Werdon and others, 2004). Metamafic rocks also occur as 100- to 300-meter-thick bands separating metasedimentary rocks. The latter group might represent tectonic stacking or alternating formation of volcanic and sedimentary sequences. Unit also contains 1–5 percent non-metamafic rocks, including granitic dikes, metasedimentary rocks, and serpentinite.

We recognize three textural types based on original grain sizes: gabbro (original grains 1–5 mm), microgabbro (original grains 0.3–1 mm), and greenstone (some phenocrysts to 1 mm, but most grains < 0.1 mm). All three textural types apparently occur as dikes or sills, but the last textural type is at least partly extrusive. Pillow textures are locally described, and Werdon and others (2004) describe basaltic conglomerate (which may be in part agglomerate). Gabbro is mostly homogeneous and always lacks foliation. Werdon and others (2004) also describe layered gabbro locally in the map area. Microgabbro and greenstone can be weakly to strongly foliated, especially near structural contacts with overlying ultramafic rocks. Finer-grained rocks are medium to dark green, and coarser-grained rocks are white and dark green to black.

The mineralogy of these rocks is complex due to partial preservation of original magmatic minerals and progressive prehnite-pumpellyite- to greenschist-facies metamorphism (with preservation of minerals from the earlier metamorphism). In at least one sample, analcite (reflecting zeolite-facies) is preserved as grains surrounded by albite. Mineralogy was determined by a combination of petrography, X-ray diffraction, and electron microprobe analyses. All rocks studied contain at least some relict augite and/or late-magmatic hornblende. Hornblende commonly replaces augite; some rocks contain only hornblende. Both are slightly to strongly altered to actinolite in most samples. Relict plagioclase was found in about half of the samples; it is partly to completely replaced by albite (always present) + prehnite + pumpellyite + chlorite + sericite + clinozoisite-epidote. In some cases, albite pseudomorphs earlier plagioclase. One-third of the samples studied contained prehnite + pumpellyite; more than half also contain actinolite, indicating progressive metamorphism (about half of the rocks contain pumpellyite, which is stable at lower greenschist-facies conditions). Actinolite was identified in three-quarters of the samples, indicating greenschist-facies conditions were commonly reached, despite the typical absence of penetrative deformation. Generally, the finer-grained samples were more thoroughly converted to non-magmatic mineral assemblages, but all gabbroic rocks—despite appearing gabbroic in hand specimen—have undergone some metamorphic overprint.

Mineral abundances in the metamafic rocks include 0–30 percent augite, 0–50 percent hornblende (likely late magmatic, commonly replacing augite), 0–45 percent plagioclase (An_{30}–An_{75}), 3–50 percent albite, 0–50 percent actinolite, 0–35 percent prehnite, 0–35 percent pumpellyite, 0–30 percent epidote-clinozoisite, 0–20 percent chlorite, 0–15 percent sericite, 0–4 percent ilmenite, 0–8 percent titanite, and 0–0.5 percent apatite. Minerals identified in less than a quarter of the samples studied include calcite (to 3 percent), magnetite (to 4 percent), pyrite (to 1 percent), and biotite (to 5 percent).

Magnetic susceptibility ranges from 0.02 to 50×10^{-3} SI, with an average of 2.8×10^{-3} SI and a median of 0.41×10^{-3} SI, and is mostly moderate to high, but quite variable, reflecting variations in alteration and the inclusion of some non-metamafic rocks (granitic dikes, metasedimentary rocks, and serpentinite) in the unit. The lower age limit is based on four $^{40}Ar/^{39}Ar$ plateau and pseudo-plateau ages (hornblende, sample 02Z135A) of 358 + 14 to 312 + 11 Ma (Werdon and others, 2004). The upper age limit is from four U-Pb zircon crystallization ages of 212.6 + 5.1 to 257.1 + 1.6 Ma (Todd and others, 2023). This unit is partly correlated with unit Pgc (greenstone and chert) of Weber and others (1978); with unit Pgb (gabbroic rocks) of Southworth (1984); and with units Mg (greenstone), Mdg (diabase and microgabbro), Mgb (gabbro), and Mgl (layered gabbro) of Werdon and others (2004).

TrMscg

METACHERT AND GREENSTONE OF THE SEVENTYMILE TERRANE (TRIASSIC TO MISSISSIPPIAN)—A poorly exposed unit that occurs intermittently with metamafic rocks in the southern and central parts of the Seventymile Terrane in the Chena map area and abundantly near the north end of the Seventymile Terrane. It is present as two moderate-sized (11–12 sq km) and several small (0.1–1 sq km) bodies intercalated with massive metamafic rocks and with non-cherty metasedimentary rocks. On average the unit is about half metachert and half greenstone, but the proportions vary widely. The two rock types can be intermingled in rubble or separated by up to hundreds of meters. The greenstones are fine-grained green rocks that could represent mafic flows, dikes, and (or) sills. Werdon and others (2004) report mafic conglomerate associated with the metachert in the southernmost exposures of the unit; this has not been observed in other locations.

The metachert comes in a variety of colors: red, green, black, and light gray are common. Color banding on the cm to mm scale is locally present. Semi-quantitative X-ray fluorescence analyses indicate the cherts contain 89–96 weight percent SiO_2, equivalent to a minimum of 80 percent silica minerals. The rocks are commonly fractured, and the metamorphism is best indicated by variable magnetic susceptibility due to partial conversion of Fe_2O_3 into magnetite.

Magnetic susceptibility (0.002–23 x 10^{-3} SI, with an average of 1.7 x 10^{-3} SI and a median of 0.13 x 10^{-3} SI) is highly variable, mostly due to differences between metachert and greenstone. Conodonts and radiolaria in metachert in the project area yield late Pennsylvanian to early Permian ages (Dusel-Bacon and Harris, 2003). Metasedimentary rocks (including metachert) in Seventymile Terrane rocks 50–150 km to the east yield ages as old as Mississippian and as young as late Triassic (Dusel-Bacon and Harris, 2003). This unit is partly correlated with unit Pgc (greenstone and chert) of Weber and others (1978), with unit Pgc (chert and greenstone) of Southworth (1984), and with unit PPc (metachert and volcaniclastic conglomerate) of Werdon and others (2004).

TrMsmg

METASEDIMENTARY ROCKS AND GREENSTONE OF THE SEVENTYMILE TERRANE (TRIASSIC TO MISSISSIPPIAN)—Metamafic rocks in this unit are like unit TrMscg, but the associated metasedimentary rocks do not include metachert. Overall, the unit is approximately two-thirds metasedimentary rocks and one-third fine-grained metamafic rocks, and likely includes sills, flows, and possible agglomerates. Locally, both components occur in the same rubble pile; more commonly, they appear as separate outcrops or float over 10–100 m. Greenstone is similar to that described for unit ŦMsmm.

The metasedimentary rocks include roughly half metaclastic rocks (metasandstone and rare metaconglomerate) and half meta-argillite. Metasandstone is mostly clast-supported, with angular to subrounded 0.2–1.5 mm grains that include abundant quartz and fine-grained, black and pale green, hard siliceous clasts (likely chert). Locally, metasandstones are matrix-supported with a sheet-silicate-rich (metawacke) or calcite-rich matrix. Elongate grains show sub-parallel alignment; metamorphism is most commonly expressed as quartz + calcite veins and veinlets. Metaconglomerate is similar but with larger clasts (0.5–4.5 cm); locally the two are observed with gradational contacts.

Most argillitic rocks possess a planar fabric and are described as either slate or phyllite. Black, gray, green, and red varieties occur; typically a single color at a given occurrence. These rocks contain 20–50 percent sheet silicates. About 20 percent lack a planar fabric, contain less than 10 percent sheet silicates and abundant (80–90 percent) quartz + albite. These siliceous rocks are pink, gray, or pale green and probably represent an impure cherty protolith.

About 20 percent of the metasedimentary rocks are located 20–150 meters from mapped felsic plutons and have been contact metamorphosed: most commonly to a pelitic hornfels, less commonly to conglomeratic hornfels (biotite-poor clasts in a biotite-rich matrix), or to calc-silicate hornfels. Pelitic hornfels is dark purple to brown, whereas calc-silicate hornfels is pale green.

Mineralogy of metasandstone and metaconglomerate includes 45–75 percent quartz (much of which is likely chert), 5–10 percent albite, 5–15 percent white mica, 5–10 percent chlorite, 0–30 percent calcite, and 0.2–1 percent rutile. Slate and phyllite contain 25–60 percent quartz, 5–45 percent albite, 5–45 percent white mica, 5–30 percent chlorite, 0–5 percent calcite, 0–2 percent carbonaceous matter, 0–5 percent hematite, and 0–1 percent rutile. Fine-grained siliceous metasedimentary rock contains 65–75 percent quartz (in part cryptocrystalline?), 10–30 percent albite, 0–7 percent white mica, 5–7 percent chlorite, 0–4 percent calcite, and 0–2 percent hematite. Pelitic hornfels contains 25–60 percent quartz, 5–25 percent plagioclase, 10–25 percent biotite, 5–10 percent muscovite, 0–15 percent andalusite, 0–7 percent cordierite, 1–3 percent ilmenite, 0.3–1 percent apatite, and 0–1 percent pyrite. Based on limited information, calc-silicate hornfels contains 20–50 percent quartz, 10–35 percent plagioclase, 10–50 percent diopside, 0–10 percent alkali feldspar, and 0–5 percent white mica.

The magnetic susceptibility of this unit ranges from 0.00 to 21×10^{-3} SI, with an average of 1.2×10^{-3} SI and a median of 0.25×10^{-3} SI, and is highly variable due to variations in the component rocks. The age is not directly determined but based on age constraints for Seventymile Terrane metasedimentary rocks elsewhere (Dusel-Bacon and Harris, 2003). This unit is correlated with unit PMv (metasandstone, meta-argillite, and greenstone) of Werdon and others (2004).

TrMsmu META-ULTRAMAFIC ROCKS OF THE SEVENTYMILE TERRANE (TRIASSIC to MISSISSIPPIAN)—An enigmatic unit mapped on top of other Seventymile assemblage units, or overlying Butte assemblage units in the southern NE Chena map; also present on top of Butte assemblage units in the central SW Chena map, and inferred (based on their strong aeromagnetic signature; Emond and MPX Geophysics, Ltd., 2022) under Quaternary sediments in the far northwestern SW Chena map. This covered group is seen as outcropping ultramafic rocks at the far western end of the aeromagnetic anomalies, 28 km west of the Chena map boundary. Unit represents more than half of the Seventymile Terrane in the project area. It occurs as numerous tiny (0.05–0.6 sq km) to small (1–4 sq km) bodies and a half-dozen larger (10–24 sq km) bodies. Based on the assumption that the basal fault is subhorizontal, Southworth (1984) reports a thickness of at least 600 m for the largest body, which is located in the southwestern NE Chena map.

Very dark green to black, and dull grayish-brown to red-brown on weathered surfaces. Black color is due to very fine-grained magnetite, which is associated with ubiquitous serpentine and occurs as disseminated crystals, especially in veins and veinlets. Typical less-serpentinized rocks (located more than 150 m from contacts with surrounding rocks) contain 3–10 mm enstatite grains that weather reddish brown and are more resistant than the surrounding dull grayish-brown-weathering olivine. Clinopyroxene (as diopside and locally augite) is essentially invisible in hand specimen but recognizable in thin section, typically with a 2–5 percent abundance. One anomalous sample contained 75 percent clinopyroxene. Enstatite abundance varies in a single exposure, but it usually accounts for 5–30 percent of these rocks, making them harzburgite. Based on petrographic and electron microprobe studies (e.g., Moshrefzadeh and Newberry, 2025), we recognize consistent mineral assemblages and compositions in these rocks. Additional minerals include Cr-Al spinel (brown translucent grains with atomic Al > Cr >> Fe3+), tiny (0.05–0.2 mm) colorless inclusions of amphibole (edenite and Mg-hornblende) in orthopyroxene, variably present minor carbonate (usually dolomite, locally calcite), and chlorite. The Mg numbers (atomic percent Mg/(Mg+Fe)) for all the minerals except spinel are high: 90–91 for olivine, 90–91 for enstatite, 92–96 for clinopyroxene, 90–95 for amphibole (mostly Cr-edenite), and 93–94 for chlorite.

Mineral abundances in these rocks include 3–90 percent serpentine, 5–80 percent olivine, 5–45 percent enstatite, 1–5 percent clinopyroxene (mostly diopside, locally augite), 1–3 percent Cr-Al spinel, 0.3–5 percent magnetite, 0–1 percent amphibole, 0–1 percent calcite or dolomite (never both together), and 0–4 percent chlorite.

A zone of silica-carbonate (magnesite and/or ankerite) 1–50 meters wide is present along the northern contact of the largest ultramafic body (Weber and others, 1978; Southworth, 1984). This intense, relatively low-temperature alteration is also locally present at the basal contact in other locations. More commonly, within about 150 m of the contact, the ultramafic rocks contain appreciable tremolite + talc + chlorite (combined abundance of 5–55 percent) in addition to serpentine. This assemblage replaces clinopyroxene to varying degrees and preferentially replaces enstatite. Thus, smaller bodies are dominated by this mineral assemblage and typically contain little or no enstatite. We consequently infer that the bulk of the meta-ultramafic rocks were harzburgite prior to metamorphism but lack direct evidence. The Cr-Al spinel characteristic of 'normal' harzburgite is locally present in these rocks but is more commonly replaced by chromite (with loss of Al and gain in Fe) and, in extreme cases, replaced by Cr-magnetite. Carbonate is nearly ubiquitous in these rocks but locally includes magnesite. Finally, pentlandite occurs as 0.03–0.06 mm disseminated grains surrounded by talc or serpentine, near altered olivine. Olivine in these rocks is commonly zoned and displays compositional variations (Mg number = 84–96) not seen in 'normal' harzburgite. Chlorite is ubiquitous and contains 0.5-4 percent Cr_2O_3, possibly derived from the destruction of Cr-Al spinel. Mineral abundances in these rocks include 15–85 percent serpentine, 5–75 percent olivine, 0.5–30 percent tremolite, 0–45 percent talc, 2–12 percent Cr-chlorite, 0–4 percent relict enstatite (mostly replaced by tremolite or talc), 0–0.5 percent clinopyroxene (mostly replaced by tremolite), 0–1 percent Cr-Al spinel + chromite, 1–5 percent magnetite (including Cr-magnetite), 0.3–12 percent carbonate (calcite or dolomite or magnesite), 0–2 percent relict hornblende (or edenite), and 0–1 percent pentlandite.

Harzburgite is generally understood to be normal mantle that has been depleted in clinopyroxene due to partial melting. Normal harzburgite in the map area was likely serpentinized by water addition along fractures under lower greenschist-facies conditions, where olivine and enstatite (both partly serpentinized) are not stable, but diopside (unaltered) is stable (Bucher and Grapes, 2011). In contrast, tremolite- and talc-altered harzburgite shows evidence for olivine formation as zoned grains and both enstatite and clinopyroxene destruction. These stabilities are consistent with upper greenschist-facies conditions (Bucher and Grapes, 2011). It is conceivable that hotter fluids (as well as higher fluid flux) were focused near the basal contact of Seventymile ultramafic rocks.

Magnetic susceptibility of the Seventymile meta-ultramafic unit is mostly high to very high and ranges from 0.07 to 63×10^{-3} SI, with an average of 14×10^{-3} SI and a median of 11 × 10^{-3} SI; variations are partly due to variations in degree of alteration to serpentine + talc. Low to very low values are from silica- and carbonate-altered rocks and quartz veins. By-and-large, however, these rocks are strongly magnetic and create strong aeromagnetic anomalies (Emond and MPX Geophysics, Ltd., 2022). Their age is problematic, as they lack zircon and amphibole with significant potassium. Assuming the harzburgite formed during the same magmatic event that produced the associated mafic rocks, we infer its age from radiometric ages of nearby gabbroic bodies (Triassic to Mississippian). Relations between the two rock types are obscure, however, and some of the dated gabbroic rocks are likely dikes (Todd and others, 2023), yielding Triassic minimum ages. This unit is correlated with unit Pu (peridotite, partly serpentinized) of Weber and others (1978); with units Psa (silica-ankerite rock), Psm (silica-magnesite rock), Psp (serpentinite), and Pu (serpentinite) of Southworth (1984); and with units Pzhd (harzburgite and dunite) and Pzs (serpentinite) of Werdon and others (2004).

Pericratonic Metamorphic Rocks

Butte Assemblage

Dusel-Bacon and others (2006) proposed the name Butte assemblage for greenschist-facies metasedimentary and lesser metavolcanic rocks that occur north of, and structurally overlying (?), amphibolite-facies rocks of the Lake George assemblage. They also indicated that Butte assemblage rocks structurally overlie those of the Blackshell assemblage and the Fairbanks-Chena assemblage. If Butte assemblage is correlative with the Totatlanika schist, and Blackshell assemblage with the Keavy Peak formation in the Alaska Range (e.g., as mapped by Wilson and others, 2015), then Butte assemblage also stratigraphically overlies the Blackshell assemblage (described below). Consequently, the regional nature of this contact is uncertain, but we have mapped it as a low-angle fault due to sharp changes in metamorphic grade and apparent truncation of Blackshell and Fairbanks-Chena assemblage lithologies in the footwall. Relatively old (202–212 ± 1 Ma) $^{40}Ar/^{39}Ar$ white mica ages determined for Butte assemblage rocks (Moshrefzadeh and others, 2026) support the notion that these rocks were metamorphosed and uplifted to high structural levels by the Late Triassic. Triassic cooling ages are uncommon in the western YTU but are found in the allochthonous Ladue River unit of the eastern YTU (Twelker and others, 2021; Jones and Benowitz, 2020).

MDbm

MARBLE, DOLOSTONE, AND CALC-SCHIST OF THE BUTTE ASSEMBLAGE (MISSISSIPPIAN to DEVONIAN)—Marble (both calcareous and dolomitic) and calcschist are widely distributed in the Butte assemblage, but less than half of the occurrences are large enough to map at a 1:100,000 scale. Typical bodies are lenticular and small (0.1–1 sq km), rarely up to 3 sq km. Tiny (<0.1 sq km) bodies in the northwest corner of the SE Chena map are taken from Werdon and others (2004). This unit comprises about 60 percent marble (70–97 percent carbonate, usually mostly calcite, but locally sub-equal or predominantly dolomite), 20 percent impure marble

(30–60 percent carbonate, usually calcite, but locally major to minor dolomite), and 20 percent calc-phyllite or calc-schist (5–20 percent calcite). Most grains in these rocks are 0.05–0.4 mm and phyllitic textures are more common than schistose textures. Marble and impure marble are white to dark gray-green; calc-phyllite is medium to dark greenish gray. All these lithologies can be banded (carbonate-rich versus carbonate-poor), but the carbonate minerals are most commonly disseminated throughout the rocks, with little carbonate banding. Both the high relative abundance of marble and impure marble and the near-absence of carbonate interlayers are in stark contrast to the Blackshell assemblage, which contains thinly interlayered calc-phyllite with lesser amounts of marble and impure marble.

Aside from carbonate minerals, Butte assemblage marble contains 0–10 percent quartz, 0–10 percent white mica, 1–8 percent chlorite, 1–10 percent albite, and 0.1–0.5 percent apatite. Impure marble contains carbonates and 5–40 percent quartz, 0–15 percent white mica, 0–20 percent chlorite, 5–20 percent albite, 0–0.5 percent apatite, and 0–1 percent titanite. Calc-phyllite contains 5–15 percent calcite, 15–55 percent quartz, 5–30 percent white mica, 5–30 percent chlorite, 5–25 percent albite, 0–20 percent alkali feldspar, 0.1–0.5 percent apatite, and 0–5 percent titanite.

About 15 percent of the calcareous Butte assemblage rocks are sufficiently close to granitic bodies to be contact metamorphosed to calc-silicate marble, calc-silicate hornfels, and skarn. Calc-silicate marble is coarser than typical Butte marble (0.5–2 mm) and contains 10–25 percent diopside and 0–10 percent plagioclase. Skarn represents marble to which significant components have been added by igneous-derived fluids. These rocks are quite diverse but generally contain 20–50 percent calcic garnet (to 5 mm) and 30–60 percent clinopyroxene (to 2 mm) with variable amounts of quartz, calcite, plagioclase, epidote, chlorite, and sulfide. Such rocks contain up to 450 ppm Cu, 250 ppm Pb, 210 ppm Sb, and 700 ppm Zn (sample 23Z236; Buchanan, Wypych, and others, 2025; NE Chena map). Butte calc-silicate hornfels is a diverse rock type, commonly with 0.5–0.6 mm grains and variable mineral banding and colors (white, green, brown). Mineralogy includes 10–60 percent diopside, 5–45 percent plagioclase, 5–20 percent biotite, 0–20 percent hornblende, 0–20 percent alkali feldspar, 0–5 percent calcite, 0–4 percent titanite, 0.5–2 percent apatite, 0–5 percent chlorite, and 0–2 percent sulfide (pyrite and/or pyrrhotite). The wide variation in mineralogy and mineral abundances mostly reflects variations in the protolith composition.

Magnetic susceptibility of this unit ranges from 0.008 to 18×10^{-3} SI, with an average of 0.44×10^{-3} SI and a median of 0.07×10^{-3} SI and is quite variable, depending on contact metamorphism. The age of this unit is constrained by Devonian-Mississippian metafelsic bodies (unit MDbf), at least some of which were hypabyssal intrusions. Unit is correlative with units Pztm (marble) and Pztc (calcschist) of the Totatlanika Schist of Smith and others (1994).

MDbf

METAFELSIC ROCKS OF THE BUTTE ASSEMBLAGE (MISSISSIPPIAN to DEVONIAN)—A texturally variable group of rocks that share a common mineralogy and a bulk composition (Buchanan, Wypych, and others, 2025) consistent with a felsic igneous protolith. These occur mostly as small (0.1–1 sq km) lenticular bodies irregularly scattered throughout the Butte assemblage. Werdon and others (2004) mapped numerous tiny (0.1–0.04 sq km) lenticular bodies and one sizeable (5.3 sq km) body in the northwest corner of the SE Chena map area. Following Werdon and others (2004) we recognize two major textural varieties: fine to medium grained (0.05–1.5 mm), and coarse porphyritic (2–15 mm alkali feldspar porphyroclasts in a 0.03–0.2 mm matrix). The former type locally contains shard-like quartz shapes suggesting a felsic tuff origin for at least some. The latter type presumably represents hypabyssal intrusions. Both types exhibit well-aligned micas and share a common mineralogy: 30–40 percent quartz, 15–40 percent alkali feldspar, 5–25 percent albite, 10–20 percent white mica, 0–5 percent biotite (metamorphic?), and 0–3 percent chlorite. Minerals only locally present include calcite (to 5 percent), ilmenite (to 1 percent), and apatite (to 0.5 percent). The high white mica content suggests that these rocks were hydrothermally altered prior to regional metamorphism, or that they represent (in part) sediments derived from felsic igneous rocks.

Magnetic susceptibility is low to very low, ranging from 0.03 to 0.3 × 10^{-3} SI, with an average of 0.11 × 10^{-3} SI and a median of 0.08 × 10^{-3} SI. Several late Devonian U-Pb crystallization ages are reported from this unit including 364 + 3 Ma (sample 96ADb24; Dusel-Bacon and others, 2006), 365.3 ± 2.1 Ma (sample 23RN513; Buchanan, Gavel, Barerra, and others, 2025), 366 ± 8 Ma (sample 20AJJ030c; Kreiner and others, 2025), and 361.1 ± 2.5 Ma (sample 76AWr287; Buchanan, Barrera, and Newberry, 2026). Given that the uncertainty in the ages extends up to earliest Mississippian, we consider the age of this unit as Mississippian to Devonian. The unit is correlated with units MDft (felsic metatuff) and Dr (metarhyolite) of Werdon and others (2004).

MDbmm

METAMAFIC ROCKS OF THE BUTTE ASSEMBLAGE (MISSISSIPPIAN to DEVONIAN)—The Butte assemblage is commonly defined by the presence of greenschist-facies metamafic rocks, which are widely distributed. About one-third of occurrences are too small to depict at 1:100,000 scale; the mapped bodies are mostly 0.1–3.5 sq km lenticular bodies. Larger (6–10 sq km) bodies are defined in part by aeromagnetic anomalies and may actually be significantly smaller. Roughly 10–15 percent of a given body consists of metasedimentary rocks, interlayered at a scale of meters to tens of meters. Textures and mineral abundances vary considerably; the common characteristics are mafic bulk compositions and arc to within-plate

(Meschede, 1986) trace-element signatures (Buchanan, Wypych, and others, 2025; Moshrefzadeh and others, 2025). These rocks are always green and commonly contain actinolite (visible in hand specimen).

About 15 percent of samples studied contain relict igneous minerals, chiefly augite and titanian augite (1–20 percent), less commonly plagioclase (0–30 percent), or hornblende (0–10 percent; all occurrences confirmed with electron microprobe). Some magnetite and ilmenite are also likely magmatic. About 15 percent of samples are better described as ‘greenstone’ and contain sufficiently abundant pyroxene or plagioclase pseudomorphs to represent originally gabbroic rocks. One sample contains quartz-filled amygdules. The remainder are strongly foliated or have hornfels textures due to proximity to plutons and their pre-metamorphic textures are unknown. Consequently, the bulk of occurrences could have been sills, dikes, flows, and (or) hypabyssal bodies.

About 80 percent of the foliated metamafic rocks are dominated by minerals with 0.02–0.2 mm grains and best described as phyllite. The remainder contain 0.05–1 mm grains (locally including biotite) and are greenschists. Oddly, calcite in both types can occur as 1–10 mm porphyroblasts that neither appear to be former plagioclase nor former vesicles.

Minerals always present in the non-hornfelsed metamafic rocks include albite (5–40 percent), chlorite (5–45 percent), epidote-clinozoisite (3–30 percent), and apatite (0.5–2.5 percent). Minerals present in most (80–90 percent of the rocks studied) include actinolite (0–60 percent), calcite (0–15 percent), and titanite (0–10 percent). Ilmenite (0–7 percent) and quartz (0–15 percent) are present in about half of the rocks. Minerals identified in 10–30 percent of samples studied include magnetite (to 5 percent) and white mica (to 10 percent). Finally, minerals rarely (about 5 percent of samples) found include biotite (to 5 percent), stilpnomelane (to 3 percent), alkali feldspar (to 2 percent), and pyrite (to 0.3 percent).

About 15 percent of samples are located sufficiently close to granitic bodies to possess contact metamorphic textures (semi-random to randomly oriented crystals) and mineralogy. The mineralogy is quite varied, as it depends on original rock composition, proximity to heat source, and degree of retrograde alteration. Crystals are generally small (0.02–0.3 mm) but hornblende can be up to 1 mm. Minerals commonly present include plagioclase (0–45 percent), albite (0–35 percent), hornblende (0–50 percent), actinolite (0–50 percent), epidote-clinozoisite (0–25 percent), apatite (0.5–2 percent), titanite (0–5 percent), ilmenite (0.5–5 percent), biotite (0–3 percent), and alkali feldspar (0–6 percent). Minerals identified in only one sample include stilpnomelane (15 percent) and diopside (30 percent); the latter in a sample less than 100 m from a large granitic body.

Magnetic susceptibility is low to very high, ranging from 0.03 to 139 × 10^{-3} SI, with an average of 3.9 × 10^{-3} SI and a median of 0.39 × 10^{-3} SI, due both to inclusion of some intermixed metasedimentary rocks into the unit and to extensive variations in magnetite content (possibly both metamorphic and pre-metamorphic) in the mafic rocks. Buchanan, Gavel, Barrera, and others (2025) report a U-Pb crystallization age of 358 ± 3 Ma (sample 23RN305), essentially straddling the Devonian-Mississippian boundary. Sample 23Z278 yielded a white mica $^{40}Ar/^{39}Ar$ age of 222.4 ± 0.9 Ma (Moshrefzadeh and others, 2026). This unit is correlated with unit MDm (greenstone) of Werdon and others (2004) and in part with unit Pzt (Totatlanika green phyllite and semischist) of Smith and others (1994).

MDbmc

METACONGLOMERATE OF THE BUTTE ASSEMBLAGE (MISSISSIPIAN to DEVONIAN)—Mostly occurs as isolated occurrences in Butte metagrit or metasedimentary units (both described below); mapped as small to large bodies (0.3–25 sq km) in the northeast and central SW Chena map area. Much of this unit was previously mapped as ‘cataclastic rocks’ by Weber and others (1978), but clasts are typically round or rounded, not angular (characteristic of cataclastic) or stretched out (characteristic of mylonites). Typical rocks are matrix-supported and contain 20–50 percent round or rounded 2 mm–40 mm quartz, feldspar, and/or granitic clasts in a schistose matrix (grain size 0.05–0.2 mm). Gradational-appearing contacts with metagrit are common, and the unit contains up to 20 percent metagrit. Granitic clasts commonly possess porphyry textures and likely represent eroded hypabyssal bodies.

Metaconglomerate mineralogy includes 45–75 percent quartz, 0–25 percent alkali feldspar, 0–20 percent albite, 3–25 percent white mica, 1–18 percent chlorite, 0–5 percent biotite, and 0.1–1 percent ilmenite. Magnetic susceptibility is low, ranging from 0.016 to 0.31 × 10^{-3} SI, with an average of 0.1 × 10^{-3} SI and a median of 0.09 × 10^{-3} SI. The unit is partly correlated with unit Pzc (cataclastic rocks) of Weber and others (1978).

MDbmg

METAGRIT OF THE BUTTE ASSEMBLAGE (MISSISSIPPIAN to DEVONIAN)—The second most abundant unit of the Butte assemblage is present throughout the Chena map area as small (1.3–4 sq km) to large (25–80 sq km) bodies. Metagrit is a metaclastic rock that displays a bimodal grain size, typically at least 5 percent 0.5–3.5 mm rounded quartz + feldspar grains in a much finer-grained (0.02–0.2 mm) matrix. It grades into metasandstone as the proportion of coarse grains drops and metaconglomerate as the size of the larger grains increases. Both commonly constitute 5–10 percent of a typical metagrit body. About 10–15 percent of metagrit occurrences are too small to depict at 1:100,000 scale and are mostly present in unit MDbms (metasedimentary rocks).

Metagrit contains 40–75 percent quartz (usually 10–20 percent are up to 3.5 mm), 5–30 percent albite (typically 5–20 percent are up to 1.5 mm), 0–20 percent alkali feldspar (typically 20–30 percent are up to 3 mm), 0–4 percent relict plagioclase (most are 0.5–0.8 mm and twinned), 7–20 percent white mica (typically 0.03–0.3 mm), and 1–20 percent chlorite (0.01–0.1 mm). A small proportion (less than 10 percent) contain 3–4 percent biotite (0.02–0.15 mm), 2–5 percent calcite (0.03–0.3 mm), 1 percent ilmenite (0.02–0.1 mm), or 1–2 percent stilpnomelane (0.02–0.1 mm).

Magnetic susceptibility is generally low and ranges from 0.00 to 0.49×10^{-3} SI, with an average of 0.12×10^{-3} SI and a median of 0.09×10^{-3} SI. The unit is partly correlated with unit MDg (metagrit and metasandstone) of Werdon and others (2004).

MDbms

METASEDIMENTARY ROCKS OF THE BUTTE ASSEMBLAGE (MISSISSIPPIAN to DEVONIAN)—The most common and extensive unit of the Butte assemblage; it occurs as 1–120 sq km regions. Mixed greenschist-facies metasedimentary unit consisting of approximately 55 percent phyllite, 7 percent schist, 15 percent metasandstone, 10 percent metagrit, 3 percent metaconglomerate, 7 percent hornfels, and approximately 1 percent each of quartzite, calcareous rocks, metafelsic rocks, and metamafic rocks. Local variations are common; for example, this unit in the western SW Chena map area is almost exclusively phyllite; in the southern part of the same map it contains at least 20 percent metaconglomerate, metasandstone, and metagrit. Many of these rock types have been broken out as separate units (MDbmc, MDbm, DMbmg), and the rocks are separately described. Most rocks in this unit are medium to dark gray or greenish gray. Phyllite and schist contain 25–85 percent sheet silicates; metasandstone typically contains less than 20 percent sheet silicates and lacks the bimodal grain size distribution that characterizes metagrit (MDbmg). Most grains in phyllite are 0.03–0.3 mm, although 1–2 percent larger (0.5–1.2 mm) quartz + feldspar 'grit' grains can be present. Schist is coarser-grained (0.05–0.7 mm) and locally contains biotite.

Phyllite, the dominant component of this unit, comprises 5–65 percent quartz, 5–35 percent albite, 3–55 percent white mica, 5–70 percent chlorite, 0.3–2 percent ilmenite, and 0.2–1 percent apatite. Minerals locally present (in 3–10 percent of the phyllite) include calcite (to 5 percent), alkali feldspar (to 10 percent), clinozoisite (to 5 percent), and carbonaceous matter (to 2 percent). Schist is mineralogically similar but contains up to 3 percent biotite and lacks carbonaceous material. Metasandstone is a quartz + feldspar-rich rock with a unimodal grain size distribution, interlayered with phyllite at scales of meters to hundreds of meters. Typically, 5–10 percent of the grains have rounded shapes. Quartz and feldspar are the coarsest grains in the rock, typically 0.2–1.2 mm, and the average grain size is generally 0.3–0.6 mm. Locally, 1–2 percent rounded, larger (1–2.5 mm) grains are present. These rocks contain 45–80 percent quartz, 5–35 percent albite, 0–35 percent alkali feldspar, 3–15 percent chlorite, 0–15 percent white mica, and 0.1–1 percent ilmenite (or rarely, rutile). About one-quarter of samples contain more than 30 percent feldspar and are distinctly arkosic. A small proportion (5–10 percent of samples) contain 1–5 percent calcite, 1–5 percent biotite, or 1–5 percent clinozoisite-epidote.

About 5–10 percent of rocks from this unit have been contact metamorphosed to fine-grained, commonly spotted, hornfels. The mineralogy varies with original bulk composition, distance from the granitic body, and degree of retrograde overprint. Texture varies with the degree of porphyroblastic minerals (andalusite or cordierite) development and the degree of recrystallization (relict textures (gritty or conglomeratic) are locally present). Virtually all contain fine-grained (0.03–0.2 mm) biotite displaying random to semi-random orientations. Consequently, most are dark-colored and can be banded, but mostly break into massive pieces. These rocks contain 1–60 percent quartz, 5–35 percent plagioclase (locally, albite instead), 5–40 percent biotite, 5–45 percent white mica (some typically possess relict parallel alignment and some display semi-random orientations), 2–20 percent sericite (as partial to nearly complete replacements of plagioclase, andalusite, and (or) cordierite), 1–25 percent chlorite (as partial replacements of biotite and (or) cordierite), and 0.1–1 percent apatite. About one-third of the hornfels samples contain identifiable andalusite (up to 15 percent and to 3 mm), cordierite (up to 25 percent and to 5 mm), or alkali feldspar (up to 5 percent and to 0.5 mm). These are commonly altered and only relicts remain. Other minerals locally present (in 10–20 percent of samples) include ilmenite (to 1 percent), clinozoisite (to 3 percent), and trace tourmaline.

Magnetic susceptibility is low to high, mostly depending on degree of contact metamorphism (which can cause magnetite or pyrrhotite formation) and inclusion of some isolated ultramafic rocks. It ranges from 0.0 to 228×10^{-3} SI, with an average of 0.69×10^{-3} SI and a median of 0.12×10^{-3} SI. Overall, magnetic susceptibility is relatively low, as reflected by the median value. This unit is correlated with undifferentiated Totatlanika schist (Pztu) in the upper Chena area (Smith and others, 1994) and with units MDsv (metasandstone, phyllite, metagrit, and graywacke) and MDc (carbonaceous phyllite and metasandstone) of the Salcha River-Pogo area (Werdon and others, 2004). A Devonian to Mississippian depositional age is inferred by association with metafelsic rocks (MDbf). Additionally, Kreiner and others (2025) report a youngest detrital zircon U-Pb age (maximum depositional age) of 350 Ma from a schist in this unit (sample 20AJJ041). A phyllite from this unit yielded a white mica $^{40}Ar/^{39}Ar$ cooling age of 202.2 ± 0.6 Ma (sample 23TJN136; Moshrefzadeh and others, 2026).

Blackshell Assemblage

Smith and others (1994) mapped a greenschist-facies carbonaceous unit and a stratigraphically underlying calcareous unit in the Upper Chena River area, which they named the Blackshell and Dan Creek units, respectively. While thick sections of calcareous rocks are often found at the apparent base of the package in the upper Chena River, we have found that calcareous rocks also occur sporadically throughout the carbonaceous rocks in the project area and their original stratigraphic position is unclear. We consequently refer to the entire package of rocks as 'Blackshell assemblage' with several units including carbonaceous and calcareous. Smith and others (1994) also mapped the contact with the structurally underlying Fairbanks-Chena assemblage as gradational, but due to the truncation of multiple lithologies, we treat this contact as a probable low-angle fault of uncertain motion.

MDblf

METAFELSIC ROCKS OF THE BLACKSHELL ASSEMBLAGE (MISSISSIPPIAN TO DEVONIAN)—A rare unit present as five tiny (0.2–0.04 sq km) bodies in the NW Chena map area and as a larger (2 sq km) body in the northwest SE Chena map area. Commonly contains 0.5–4 percent iron oxide pseudomorphs of pyrite, relatively abundant white mica (10–25 percent), and anomalously abundant (40–70 percent) quartz, suggesting that they were quartz-sericite-pyrite altered prior to metamorphism. Some of the quartz is present as 3–7 mm porphyroclasts representing igneous grains. Some (0–30 percent) alkali feldspar (0.01–5.5 mm, some porphyroclasts) and albite (0–12 percent, 0.05–6 mm, some porphyroclasts) are also variably present. Small amounts (0–2 percent) of chlorite are locally present. Anomalous Ba (up to 1.7% BaO; Buchanan, Wypych, and others, 2025) is locally present as unknown minerals. These rocks could represent altered rhyolitic tuff and/or small hypabyssal felsic intrusions.

In contrast, the 2 sq km body in the SE Chena map area is less altered, with a granitic mineralogy and porphyroclastic textures (quartz and alkali feldspar to 2 cm; Lessard, 2006). Average modal mineralogy includes 45 percent quartz, 35 percent alkali feldspar, 15 percent albite, 5 percent muscovite and less than 0.5 percent accessory minerals (Werdon and others, 2004). This body was likely a hypabyssal intrusion.

Magnetic susceptibility is low to very low; it ranges from 0.02–0.17 x 10^{-3} SI, with an average of 0.09 x 10^{-3} SI and a median of 0.08 x 10^{-3} SI but is based on a small number of measurements. Dusel-Bacon and others (2006) give three U-Pb crystallization ages of 353 ± 7 to 372 ± 5 Ma for this unit in the Chena map area. Buchanan, Barrera and others (2025) give a U-Pb crystallization age of 361.3 ± 2 Ma (23JWB090) for a felsic metatuff(?) in the south-central part of the NW Chena map area. This unit correlates with metarhyolite (Dr) of Werdon and others (2004).

pMbl

CARBONACEOUS ROCKS OF THE BLACKSHELL ASSEMBLAGE (PRE-MISSISSIPPIAN)—The most widespread unit of Blackshell; it occurs in all four Chena map areas, although least commonly in the SE Chena map. Includes small amounts of non-graphitic and calcareous rocks in occurrences too small to depict at 1:100,000 scale. The unit is approximately one-third graphitic quartzite and two-thirds graphitic phyllite. Both are black to very dark gray, fine-grained rocks with most grains 0.02–0.15 mm.

Graphitic quartzite occurs as massive to slightly phyllitic rock with 80–95 percent quartz, 2–15 percent white mica, 0–5 percent albite, 1–8 percent graphite or carbonaceous matter, 0.2–4 percent apatite, 0–7 percent chlorite, and 0–1 percent ilmenite.

Graphitic phyllite is fissile and easily eroded; it contains 10–60 percent quartz, 25–60 percent white mica, 1–30 percent albite, 1–5 percent graphite (or carbonaceous matter), 0.2–9 percent apatite, 2–25 percent chlorite, 1–2 percent ilmenite, and (locally) 0–3 percent biotite. Relatively high white mica:chlorite ratios and locally anomalous (0.34–3.5 percent) P_2O_5 and (or) BaO (0.2–0.9 percent; Buchanan, Wypych, and others, 2025) are distinctive.

About one-quarter of graphitic phyllite occurrences are close enough (within a kilometer) to granitic bodies to be contact metamorphosed to pelitic hornfels. The mineralogy of such rocks depends on the original bulk composition, proximity to intrusion, and degree of retrograde overprint. All are characterized by sheet silicates displaying random or semi-random orientations; many possess distinctive 2–4 mm porphyroblasts. Mineral abundances include 5–60 percent quartz (0.02–2.5 mm), 2–55 percent white mica (0.02–1.5 mm, finer grains partly replace plagioclase, cordierite, and (or) andalusite), 0–35 percent biotite (0.01–0.4 mm), 0–70 percent poikilitic cordierite (0.1–4 mm, some partly replaced by chlorite + white mica), 0–25 percent euhedral andalusite (0.1–3 mm, partly replaced by white mica), 0–35 percent low-calcium amphibole (both anthophyllite and cummingtonite occur), 0–25 percent alkali feldspar (0.03–2.5 mm, some porphyroblastic), 0–35 percent chlorite (0.2–0.5 mm, mostly alteration of biotite and cordierite), 0–2 percent ilmenite (0.01–0.15 mm), 0.2–1 percent apatite (0.02–0.1 mm), and 0–5 percent euhedral magnetite (0.02–0.3 mm). These rocks commonly contain up to 1 percent BaO (Buchanan, Wypych, and others, 2025), reflecting the graphitic phyllite protolith.

Magnetic susceptibility of this unit ranges from 0.004 to 34×10^{-3} SI, with an average of 0.23×10^{-3} SI and a median of 0.06×10^{-3} SI. It is mostly low but variable; contact metamorphism causes elevated values. The age of this unit is constrained by Devono-Mississippian metafelsic bodies, at least some of which were hypabyssal intrusions. This unit is correlative with unit Pzq (quartzite, meta-argillite, and phyllite) of Weber and others (1978) and Foster and others (1983); with unit Pzbp (Blackshell quartzite and phyllite) of Smith and others (1994); with unit Dbs (Birch Hill slate and quartzite) of Newberry and others (1996); and with unit MDc (carbonaceous phyllite and meta-sandstone) of Werdon and others (2004).

pMblc

CALC-PHYLLITE AND MARBLE OF THE BLACKSHELL ASSEMBLAGE (PRE-MISSIPPIAN)—This unit accounts for approximately one-quarter of the Blackshell assemblage. In the east-central part of the project area it constitutes the structurally lowest part of the assemblage, but this stratigraphic relationship is not apparent elsewhere. Mostly these rocks are present as 0.5–11 sq km lenses in unit pMbl. This unit is approximately 75 percent calc-phyllite (locally calc-schist) with 3–40 percent carbonate minerals (usually calcite, but locally dolomite dominates). About 15 percent of this unit is impure marble (40–55 percent carbonate, almost always calcite); about 10 percent is marble, with 65–90 percent calcite.

Blackshell calc-phyllite and most marble contains 0.05–0.4 mm grains; calc-schist is coarser-grained (0.1–1 mm) and more commonly contains biotite, in addition to chlorite and white mica. For both the typical texture consists of alternating silicate-rich and carbonate-rich bands, each 0.03–3 mm thick. Rocks with lower carbonate abundances contain relatively thinner carbonate-rich bands combined with thicker silicate-rich bands. Besides carbonates, minerals present in calc-phyllite include 10–65 percent quartz, 5–35 percent white mica, 2–30 percent chlorite, 5–25 percent albite, 0.2–1 percent apatite, and 0–3 percent graphite. Calc-schist has similar mineralogy and abundances but contains up to 5 percent biotite.

Impure Blackshell marble contains 40–55 percent calcite, 0–15 percent dolomite, 10–15 percent quartz, 5–20 percent white mica, 3–15 percent chlorite, 5–20 percent albite, 0.2–1 percent apatite and 0–1 percent graphite. Marble contains 65–90 calcite, 0–15 percent quartz, 0–10 percent white mica, 0–10 percent chlorite, 5–20 percent albite, and 0.5 percent apatite.

About one-third of the exposures of this unit are contact metamorphosed, commonly to a distinctive banded pale green calc-silicate/silicate hornfels, less commonly to massive calc-silicate rock or skarn. These mineralogical bands reflect compositional banding in the calc-phyllite protolith. Sheet silicates and amphiboles display random to semi-random orientations within the bands. Most grains in calc-silicate hornfels are 0.05–0.5 mm, but diopside and actinolite can be as large as 1.5–2.5 mm. Variations in mineralogy and abundances in calc-silicate hornfels reflect original rock compositional variations, distance from pluton, and degree of retrograde overprint. Diopside and plagioclase are the only minerals consistently present. Mineralogy includes 0–60 percent quartz, 5–30 percent plagioclase, 5–50 percent diopside, 0–25 percent biotite, 0–70 percent actinolite (in part a replacement of diopside), 0–30 percent clinozoisite-epidote, 0–7 percent white mica (in part replacing plagioclase), 0–15 percent alkali feldspar, 1–3 percent titanite, 0–35 percent wollastonite (variably present in rocks within a few hundred meters of an intrusion), 0–5 percent calcite (most likely secondary), 0–2 percent ilmenite, 0.1–1 percent apatite, 0–5 percent chlorite (some secondary), and 0–4 percent pyrrhotite + pyrite. These rocks are only weakly anomalous in metallic elements (Buchanan, Wypych, and others, 2025; Moshrefzadeh and others, 2025).

Blackshell skarn occurs as pods of massive calc-silicates that likely represent metasomatized Blackshell marble or impure marble, located within 250 m of granite contacts. The grain size is typically 0.4–5 mm, and the rocks are dominated by dark-colored calcic garnet and hedenbergite (Fe-rich) clinopyroxene. Anomalous concentrations of W (to 0.1%), Bi (to 645 ppm), Ag (to 4 ppm), As (to 300 ppm), Sn (to 290 ppm), Zn (to 300 ppm), and Sb (to 75 ppm) are present (Buchanan, Wypych, and others, 2025). Typical mineralogy includes 0–15 percent quartz, 5–45 percent calcic garnet, 30–60 percent hedenbergite, 0–15 percent vesuvianite, 0–25 percent epidote (mostly replaces garnet), 0–2 percent actinolite (replaces hedenbergite), 0–0.5 percent chlorite (partly replaces garnet), 0–20 percent calcite (mostly relict from marble, but some likely retrograde), 0–1 percent titanite, 0–0.2 percent scheelite, and 0.2–8 percent sulfide (mostly pyrrhotite with lesser pyrite and minor to trace sphalerite, chalcopyrite, and bismuthinite). Microprobe analyses indicate up to 2.5 percent SnO_2 in epidote and up to 2.4 percent SnO_2 in titanite. Minerals locally present include biotite (to 10 percent), alkali feldspar (up to 4 percent), and apatite (up to 0.5 percent).

Magnetic susceptibility of this unit ranges from 0.011–5.4 x 10^{-3} SI, with an average of 0.24 x 10^{-3} SI and a median of 0.14 x 10^{-3} SI and is quite variable depending on contact metamorphism and metasomatism. Otherwise, the values are low to very low. The age of this unit is constrained by late Ordovician to mid-Devonian corals found in calc-phyllite float in the upper Chena drainage, south-central Circle quadrangle (Smith and others, 1994). This unit broadly correlates with unit |m (phyllite, calcareous phyllite, and marble) of Weber and others (1978) and Foster and others (1983), units Pzbc, Pzdc, Pzdp, and Pzdm (calcareous rocks of Blackshell and Dan Creek units) of Smith and others (1994), and with unit Dbcs (calcareous schist and impure marble) of Newberry and others (1996).

pMblq

QUARTZITE AND QUARTZ PHYLLITE OF THE BLACKSHELL ASSEMBLAGE (PRE-MISSIPPIAN)—This rare unit (about 5 percent of Blackshell assemblage) consists of rocks that are neither carbonaceous nor calcareous, mostly present as narrow (0.1–3.5 sq km) lenses in carbonaceous Blackshell. On average, about one-third of the unit is quartzite and two-thirds quartz phyllite. Both are pale gray and typically have grain sizes of 0.02–0.4 mm. Quartzite contains 80–90 percent quartz, 5–7 percent white mica, 0–7 percent chlorite, 3–7 percent albite, 0–0.5 percent apatite, and 0–0.5 percent ilmenite. Quartz phyllite contains 60–75 percent quartz, 7–30 percent white mica, 1–5 percent chlorite, 5–15 percent albite, 0.3–1 percent ilmenite, and 0.1–0.5 percent apatite.

Magnetic susceptibility of this unit is generally low and ranges from 0.02 to 0.45 × 10^{-3} SI, with an average of 0.14 × 10^{-3} SI and a median of 0.09 × 10^{-3} SI. I. Age is based on age constraints for Blackshell graphitic rocks (unit pMbl). Although previous workers (e.g., Smith and others, 1994) describe pale colored, non-calcareous rocks in graphitic Blackshell, this unit has not previously been broken out and is not directly correlated with other units in Interior Alaska.

Ordovician Meta-ultramafic and Metamafic Rocks

Omum META-ULTRAMAFIC AND METAMAFIC ROCKS (EARLY ORDOVICIAN) –An enigmatic unit found as one tiny (0.06 sq km) sliver located between rocks of the Butte and Blackshell assemblages near the southeast corner of the NW Chena map. Unit was previously identified as unit Pu (that is, ultramafic rocks of the Seventymile terrane) by Weber and others (1978). It contains roughly half metagabbroic and half meta-ultramafic rocks. Metamorphic conditions are mid- to upper-greenschist-facies with a distinct lack of penetrative deformation fabric. Relative to Seventymile terrane meta-ultramafic rocks, the ultramafic rocks of this unit contain 5–50 times as much TiO_2, P_2O_5, and rare earth element concentrations and 10–80 times as much Nb and Zr (Buchanan, Wypych, and others, 2025). They also contain significantly less MgO and more Fe_2O_3 (Buchanan, Wypych, and others, 2025). Metagabbroic rocks of this unit contain 2–5 times as much Nb as metamafic rocks of the Seventymile terrane (Buchanan, Wypych, and others, 2025). Based on relative Zr, Nb, and Y concentrations, both meta-ultramafic and metamafic rocks of this unit plot in the 'within-plate' field of Meschede (1986) as opposed to Seventymile metamafic rocks, which plot in the mid-ocean ridge basalt field.

Metagabbroic rocks are pale and dark green and were originally medium to coarse grained (0.3–3.5 mm); plagioclase is completely pseudomorphed by albite + chlorite + clinozoisite + sericite + calcite. Relict diopside crystals up to 3.5 mm in diameter were first partly replaced by (late magmatic) brown pleochroic hornblende with up to 2.5 percent TiO_2 and 1 percent K_2O (electron microprobe analyses). Hornblende and especially diopside were subsequently replaced by actinolite + chlorite. Relict ilmenite crystals (up to 0.8 mm) are partly to mostly replaced by pseudomorphic titanite up to 1.5 mm. Small (up to 0.2 mm) biotite grains, partly altered to chlorite, are likely late magmatic. Apatite crystals to 0.1 mm are scattered throughout. Mineral abundances (based on one sample) include 10 percent diopside, 10 percent hornblende, 3 percent biotite, 2 percent ilmenite, 1 percent apatite, 25 percent actinolite, 30 percent albite, 4 percent titanite, 7 percent clinozoisite, 2 percent sericite, and 5 percent chlorite.

Metamafic rocks are fine- to medium-grained, greenish-black. They are composed almost entirely of secondary minerals with the exception of late magmatic (?) brown pleochroic hornblende (with up to 3.5 percent TiO_2 and 0.8 percent K_2O) relicts up to 1 mm. Fine-grained aggregates of serpentine, talc, or actinolite to 1 mm suggest former olivine and clinopyroxene. Rare, partly chloritized, biotite grains may also be of late magmatic origins. Subhedral ilmenite (to 0.7 mm) and rare apatite (to 0.15 mm) are both likely magmatic and not identified in Seventymile terrane meta-ultramafic rocks. Green pleochroic chlorite abundantly occurs as 0.05 mm scaley aggregates that appear to have replaced an unknown interstitial mineral or minerals. Secondary dolomite and pyrrhotite are also variably present. Mineral abundances include 0–7 percent hornblende, 0–0.5 percent biotite, 0.5–1 percent ilmenite, 2–5 percent Cr-magnetite (some after chromite?), 35–40 percent serpentine, 30–35 percent chlorite, 0–20 percent actinolite, 0–25 percent talc, 0–2 percent dolomite, 0–0.5 percent pyrrhotite, and 0.2 percent apatite.

Based on a small sample set, the magnetic susceptibility of metagabbro ranges from 0.4 to 0.7×10^{-3} SI, with an average and median of 0.57×10^{-3} SI. Meta-ultramafic rocks are much more magnetic, ranging from $25–88 \times 10^{-3}$ SI, with an average of 62×10^{-3} and a median of 70×10^{-3}. The age of this unit is based on a U-Pb zircon crystallization age of 480.8 ± 1.4 Ma (sample 23JWB125; Buchanan, Barrera, and others, 2025). The best correlation based on age and lithology is with unit Pzmi (mafic-ultramafic intrusions associated with early Ordovician Fossil Creek volcanics) of Smith and others (1987), located 100 km to the north of the Chena map area; if true, this has important tectonic implications.

Preacher Assemblage

Smith and others (1987) recognized a metagrit-bearing unit, which they identified as 'lower metagrit', located structurally between Fairbanks schist and the latest Proterozoic to mid-Cambrian (Dusel-Bacon and others, 2017) Wickersham units (located about 50 km northwest of the Chena map area). Smith and others (1987) noted several differences between this assemblage and the structurally overlying Wickersham units, including the presence of marble and chlorite-rich schist or phyllite. We rename this assemblage after prominent exposures in the upper Preacher Creek area of the Circle Quadrangle. The metamorphic grade of the Preacher assemblage is mid- to upper-greenschist, based on the presence of albite (instead of plagioclase), variable presence of biotite, and absence of garnet. The age of the Preacher assemblage is poorly constrained. If it stratigraphically (as well as structurally) underlies the Wickersham grit (Smith and others, 1987), then it must be older than mid-Cambrian.

The contact with the structurally underlying Fairbanks-Chena assemblage rocks is considered a low-angle fault with uncertain motion because it appears to cut off units on both sides. The location of this fault is locally uncertain because Fairbanks-Chena assemblage rocks tend to be strongly retrograded in the vicinity of the fault contact and are difficult to distinguish from Preacher assemblage. Preacher assemblage rocks are restricted to the northern parts of the NW Chena and NE Chena maps.

PzƵpcm

CALC-SCHIST AND MARBLE OF THE PREACHER ASSEMBLAGE (PALEOZOIC TO NEOPROTEROZOIC)—This relatively rare unit accounts for about 5 percent of the Preacher assemblage in the map area. It is mostly present as small (0.2–1.2 sq km) lenses and one larger (12 sq km) layer. Based on limited exposures, about one-third of the unit is marble, one-third is impure marble, and one-third is calc-schist or calc-phyllite. Calc-phyllite has mostly 0.05–0.5 mm grains (but locally with 0.5–1 mm quartz porphyroclastic 'grit' grains) and lacks biotite. Calc-schist is coarser-grained (0.1–2 mm) and locally contains biotite. Preacher marble and impure marble generally have grain sizes closer to those of calc-phyllite. All the rocks are white to pale greenish gray on fresh surfaces.

Preacher assemblage marble contains 65–90 percent carbonate (usually calcite, but locally with sub-equal calcite and dolomite), 0–5 percent quartz, 0–10 percent white mica, 0–10 percent chlorite, 5–10 percent albite, 0.1–0.5 percent titanite, and trace apatite. Impure marble contains 35–55 percent carbonate (usually calcite, but locally dolomite), 25–45 percent quartz, 0–15 percent white mica, 4–7 percent chlorite, 5–25 percent albite, and trace titanite and apatite. Calc-phyllite and calc-schist contain 5–20 percent carbonate (usually calcite, but locally subequal dolomite and calcite), 20–55 percent quartz, 5–12 percent white mica, 7–20 percent chlorite, 0–5 percent alkali feldspar, 15–35 percent albite, 0–3 percent biotite, 0.2–1 percent titanite, and 0.2–1 percent apatite. Carbonate banding in these rocks is weakly present; much of the carbonate is instead scattered throughout the rock.

Magnetic susceptibility of this unit is generally low and ranges from 0.00 to 0.46×10^{-3} SI, with an average of 0.11×10^{-3} SI and a median of 0.06×10^{-3} SI. Marble values are very low; impure marble and calc-schist are higher. This unit is correlated with marble (unit pꞒm) of the lower metagrit unit of Smith and others (1987).

PzƵpcp

CHLORITIC SCHIST AND PHYLLITE OF THE PREACHER ASSEMBLAGE (PALEOZOIC TO NEOPROTEROZOIC)—A rare (less than 0.5 percent of the Preacher assemblage in the project area) but important unit, as it is lithologically distinctive. Green to grayish green in hand specimen, this unit consists of chlorite-rich rocks that superficially resemble metamafic rocks, but contain too much quartz (20–60 percent) and white mica (5–15 percent) to possess mafic protoliths. Major-element analyses (Moshrefzadeh and others, 2025) indicate 58–78 percent SiO_2 and 0.7–3.9 percent CaO, which are too high and low, respectively, for mafic rocks. Chloritic phyllite, the more common variety, displays most grain sizes of 0.02–0.3 mm (with porphyroblastic albite locally to 1 mm) and variable (0–1.5 percent) biotite. Chloritic schist is coarser, with most grains 0.05–0.5 mm and porphyroblastic albite to 2.5 mm, and consistently biotite-bearing (2–4 percent). The two have otherwise similar mineralogy, containing 20–60 percent quartz, 5–35 percent albite, 5–15 percent white mica, 20–45 percent chlorite, 0–10 percent clinozoisite, 0–7 percent calcite, 0–5 percent titanite, 0–2 percent ilmenite, with variably trace apatite and tourmaline.

Based on a small sample set, the magnetic susceptibility of this unit is low and ranges from 0.1 to 0.15 × 10^{-3} SI, with an average and median of 0.12 × 10^{-3} SI. This unit is correlated with chloritic schist (unit p€c) of the lower metagrit unit of Smith and others (1987) and unit Pzcl (chlorite schist) of Wiltse and others (1995). It also correlates in part with metasedimentary parts of unit Pzp€m (mafic schist) of Foster and others (1983).

PzPpmm

METAMAFIC ROCKS OF THE PREACHER ASSEMBLAGE (PALEOZOIC TO NEOPROTEROZOIC)—Another rare (approximately 0.1 percent of the Preacher assemblage in the Chena map area) but distinctive unit, present as 0.2–0.4 sq km lenses in the schist and phyllite unit (PzPpsp). Rocks are green, green and white, or grayish green and have phyllitic textures, locally with porphyroblastic albite. Typical grain size for most minerals is 0.03–0.3 mm; albite is up to 0.8 mm. Mineralogy includes 0–10 percent quartz, 20–30 percent albite, 15–45 percent chlorite, 5–25 percent clinozoisite-epidote, 1–9 percent calcite, 1–4 percent titanite, 0.5–1.5 percent apatite, 0–25 percent actinolite, 0–4 percent white mica, 0–1 percent ilmenite, and 0–3 percent alkali feldspar.

Based on a small sample set, the magnetic susceptibility of this unit ranges from 0.33 to 0.64 × 10^{-3} SI, with a mean and median of 0.44 × 10^{-3} SI. This unit is partly correlated with unit Pzp€m (mafic schist) of Foster and others (1983).

PzPpsp

SCHIST AND PHYLLITE OF THE PREACHER ASSEMBLAGE (PALEOZOIC TO NEOPROTEROZOIC)—A common (about 15 percent of the assemblage in the Chena map area) unit present interlayered with or as 0.5–5 sq km lenses in the predominant metasandstone and metagrit unit (PzPpsg). About one-third of the rocks are phyllite (most grains 0.05–0.3 mm) that lack biotite, and two-thirds are schist (most grains 0.1–1 mm) that variably contain biotite and especially porphyroblastic albite (locally to 1.5 mm). The phyllite contains 5–75 percent quartz, 5–25 percent albite, 10–60 percent white mica, 5–30 percent chlorite (but with white mica always more abundant than chlorite), 0–3 percent ilmenite, and trace tourmaline. Calcite (to 2 percent), magnetite (to 2 percent), clinozoisite (to 1 percent), and apatite (to 1 percent) are locally present. Supergene iron oxide staining along foliation surfaces is relatively common. Schist has the same mineralogy but also contains biotite (0–15 percent) and locally alkali feldspar (to 10 percent).

Magnetic susceptibility of this unit is generally low and ranges from 0.03 to 0.4 × 10^{-3} SI, with an average of 0.15 × 10^{-3} SI and a median of 0.14 × 10^{-3} SI. This unit is correlated with pelitic schist of the lower grit (unit p€sg) of Smith and others (1987).

PzPpsg METASANDSTONE AND METAGRIT OF THE PREACHER ASSEMBLAGE (PALEOZOIC TO NEOPROTEROZOIC)—The most abundant (80 percent) Preacher assemblage unit in the Chena map area, this unit is approximately 85 percent metaclastic rocks and 15 percent schist or phyllite (previously described). We define metagrit as a metaclastic rock displaying a bimodal grain-size distribution, with at least 5 percent coarser grains in a finer-grained matrix. About half of the Preacher metaclastic rocks are metagrit, and the other half are metasandstone.

Preacher assemblage metagrit contains 5–30 percent coarse (0.8–3.5 mm) rounded quartz + feldspar grains in a 0.03–0.3 mm matrix of quartz, feldspar, and sheet silicates + calcite. The mineralogy includes 40–80 percent quartz, 5–20 percent albite, 0–7 percent alkali feldspar, 5–15 percent white mica, 1–5 percent chlorite, 0–25 percent calcite, and 0–5 percent biotite. Locally occurring minerals include apatite (to 1 percent) and ilmenite (to 1 percent). Supergene iron oxide coatings are relatively common.

Metasandstone typically consists of 0.05–0.45 mm grains; some quartz grains are rounded, most are anhedral. Mineralogy includes 60–80 percent quartz, 5–15 percent albite, 8–12 percent white mica, 5–8 percent chlorite, and 0–3 percent biotite.

Magnetic susceptibility of this unit is low and ranges from 0.007 to 0.29×10^{-3} SI, with an average of 0.09×10^{-3} SI and a median of 0.07×10^{-3} SI. This unit is correlated with unit Pzp€gr (grit and quartzite) of Foster and others (1983) and with lower grit (unit p€sg) of Smith and others (1987).

Fairbanks-Chena Assemblage

Dusel-Bacon and others (2006) named the (mostly) amphibolite-facies rocks that occur north of the greenschist-facies belt (Butte and Blackshell assemblages) “Fairbanks-Chena assemblage.” They noted that this assemblage contains more quartzite and calcareous rocks and less orthogneiss than the Lake George assemblage. The metamorphic grade of the Fairbanks-Chena assemblage appears to be epidote-amphibolite (Newberry and others, 1996); Lake George is of higher, upper amphibolite-facies as evidenced by the common occurrence of garnet and local diopside in metamafic rocks (Newberry and Twelker, 2021). Newberry and Moshrefzadeh (2026) have shown that amphibolite hornblende and plagioclase compositions contrast between the two different assemblages; we use this to further distinguish between Fairbanks-Chena and Lake George assemblage.

We identified several areas of Fairbanks-Chena assemblage in the Goodpasture mining district where Lake George assemblage was previously mapped (Dusel-Bacon and others, 2006), based on amphibolite mineral compositions (Newberry and Moshrefzadeh, 2026) and the presence of rocks of somewhat lower metamorphic grade and with a greater abundance of quartzite and calcareous rocks and lower abundance of orthogneiss than is typical of Lake George assemblage. The two assemblages appear to be in low-angle fault contact, with Lake George assemblage in the footwall. This structural relationship is supported by hornblende $^{40}Ar/^{39}Ar$ metamorphic cooling ages as old as 181 ± 6.5 Ma (Dusel-Bacon and others, 2002) locally reported from amphibolites in this assemblage, which is considerably older than hornblende from the underlying Lake George assemblage.

TrPzfcu META-ULTRAMAFIC ROCKS OF FAIRBANKS-CHENA ASSEMBLAGE (TRIASSIC? TO PALEOZOIC)—Ten tiny (0.04–0.1 sq km), sinuous bodies and one small (2 sq km) body sporadically occur in the Fairbanks-Chena assemblage. Most of these are in the southwestern part of the SE Chena or the northern or western parts of the NE Chena map; one is in the western part of the NW Chena map. These are amphibolite-facies metamorphosed ultramafic rocks occurring as lenses mostly within the Fairbanks-Chena schist and gneiss (unit pMfcsg). Locally, bodies occur adjacent to Fairbanks-Chena amphibolite, and the bodies include up to 10 percent amphibolite.

Margins of larger bodies (and smaller bodies entirely) are strongly retrograded to serpentine (20–85 percent), talc (0–60 percent), chlorite (0–60 percent), magnetite (2–10 percent), and magnesite and/or dolomite (1–33 percent). Less-retrograded rocks occur towards the interiors of bodies and typically contain 35–80 percent olivine, 5–15 percent tremolite, 0–10 percent talc, 0.1–7 percent anthophyllite, 1–7 percent chlorite, 2–30 percent serpentine, 1–2 percent magnetite, 0.5–2 percent chromite, and 0–1.5 percent calcite and/or dolomite. These minerals were confirmed by microprobe (this study).

The assemblage anthophyllite + forsterite + chlorite + tremolite is only stable under amphibolite-facies conditions, and the occurrence of this assemblage implies that the ultramafic rocks were metamorphosed with the enclosing Fairbanks-Chena assemblage rocks.

Magnetite contents are relatively high (1–10 percent) but depend on the amount of low-Fe (talc and serpentine) mineral destruction of higher-Fe (olivine and anthophyllite) minerals. Consequently, the magnetic susceptibility of this unit is higher than that of any other unit in the Fairbanks-Chena assemblage. However, because the unit in part contains poorly magnetic ultramafic rocks and some non-ultramafic rocks, the magnetic susceptibility ranges from 0.12 to 83 × 10^{-3} SI, with an average of 18 × 10^{-3} SI and a median of 9.5 × 10^{-3} SI and is variably high. In part, the contacts of this unit are based on magnetic highs seen on aeromagnetic maps (Burns and others, 2020).

The occurrence of amphibolite-facies metamorphic assemblages (including anthophyllite) indicates that the meta-ultramafic rocks were present, likely through structural incorporation, before amphibolite-facies metamorphism. The only known source of ultramafic rocks in Interior Alaska is the Mississippian to Upper Triassic

Seventymile terrane, typically 30–55 km to the south, but how such rocks were slivered into the Fairbanks-Chena assemblage is unknown. Furthermore, Fairbanks-Chena assemblage meta-ultramafic rocks contain much higher immobile element concentrations than Seventymile ultramafic rocks. For example, they contain more than 10 times as much TiO_2, Ce, and Zr and 7–8 times as much Nb and Y (Moshrefzadeh and others, 2025). Thus, correlation of the meta-ultramafic rocks with the less-metamorphosed meta-ultramafic rocks of the Seventymile assemblage is uncertain. This unit correlates with unit Pzu (ultramafic rocks) of Weber and others (1978), Pzp (serpentinized peridotite) of Foster and others (1983) and with unit TPzfcu of Twelker and others (2025).

MDcag

CENTRAL CREEK AUGEN ORTHOGNEISS (EARLY MISSISSIPPIAN TO LATE DEVONIAN)—Comprises a large (345 sq km) body in the southern SE Chena map and numerous smaller (0.3–12 sq km) bodies in the NE Chena and especially the SE Chena maps. Unit is approximately 80 percent granite orthogneiss, 5 percent other metaigneous rocks (non-granite orthogneiss and minor amphibolite), 10 percent metasedimentary rocks (paragneiss and lesser schist), and 5 percent igneous dikes of various compositions and likely ages. Of the granite orthogneiss, approximately 85 percent displays 2–20 percent alkali feldspar megacrysts (“augen”), mostly 1–4 cm long, locally up to 6 cm. The unit is commonly white to light brown and has experienced minor to major weathering. Gneissic matrix is fine- to coarse-grained (0.1–3 mm); micas commonly form foliation-parallel, millimeter-scale bands that separate felsic layers. Typical mineralogy for both augen-bearing and augen-free granite orthogneiss includes 20–35 percent subhedral to anhedral alkali feldspar, 20–30 percent subhedral to anhedral plagioclase, 25–40 percent granoblastic quartz with irregular grain boundaries and common sub-grains, 5–15 percent biotite, and 2–10 percent muscovite. Plagioclase is slightly altered to sericite, and biotite is variably altered to chlorite. Minor minerals include up to 2 percent garnet, 1 percent clinozoisite, 5 percent chlorite, 0.1 percent tourmaline, 0.5 percent titanite, and trace opaque minerals, apatite, and zircon. We interpret the minor metasedimentary rocks in this unit as former inclusions in, or screens between, megacrystic granite bodies. Magnetic susceptibility is mostly low (0.0–3.3 x 10^{-3} SI, with an average of 0.18 x 10^{-3} SI and a median of 0.11 x 10^{-3} SI), reflecting the predominance of granitic orthogneiss.

Aleinikoff and others (1986) report two U-Pb crystallization ages of 341–344 Ma, and Dusel-Bacon and others (2006) report five additional U-Pb crystallization ages of 361± 5 to 371 ± 3 Ma for the Central Creek orthogneiss body (SE Chena map). Dusel-Bacon and others (2006) also report a U-Pb crystallization age of 355 ± 4 Ma for a small augen gneiss body about 14 km NW of West Point, in the east-central NE Chena map area. This unit is correlated with unit Pzra (augen gneiss in the Chena River sequence) of Smith and others (1994), with unit Mog (orthogneiss) of Newberry and others (1996) and partly with unit PzpЄa (augen gneiss) of Weber and others (1978). It is distinguished from Divide Mountain augen orthogneiss (unit MDag, Wypych and others, 2021) by association with the Fairbanks-Chena assemblage, including amphibolites metamorphosed to epidote-amphibolite facies (unit MDfca).

MDfca

AMPHIBOLITE OF FAIRBANKS-CHENA ASSEMBLAGE (MISSISSIPPIAN to DEVONIAN)—Amphibolite to amphibole-rich orthogneiss is commonly present with other Fairbanks-Chena lithologies. It occurs as narrow discontinuous lenses throughout the Fairbanks-Chena schist and gneiss unit, and as individual occurrences too small to map. Unit is mostly amphibolite, with minor (10–15 percent) other Fairbanks-Chena assemblage lithologies, mostly schist or gneiss. Rocks are dark green to gray, commonly weathered to brown, and are fine to coarse-grained with a gneissic to schistose texture. The predominant rock type is biotite-hornblende amphibolite (some partially retrograded to greenschist-facies) with a 0.1–4 mm grain size. Thin section examination shows that epidote-clinozoisite (not visible in hand specimen) is nearly ubiquitous, with 2–10 percent typical. Other minerals typically present include 40–75 percent hornblende (subhedral, 0.2–4 mm), 15–45 percent subhedral plagioclase (0.1–2.5 mm) partly altered to sericite (0.2–3 percent), 0–10 percent biotite (0.1–2 mm), 0.5–3 percent subhedral to euhedral titanite (0.03–0.3 mm), 0–3 percent calcite (mostly anhedral, 0.0.1–0.8 mm), 0–5 percent anhedral quartz (0.02–0.7 mm), 0.3–2 percent euhedral apatite (0.03–0.2 mm), 0–3 percent chlorite (subhedral grains and aggregates, 0.02–0.3 mm), and 0.2–5 percent opaques (ilmenite + magnetite). Based on microprobe analyses, the plagioclase is An_{20-40}, although most samples display only a portion of that range (Newberry and Moshrefzadeh, 2026). A small number of samples contain 3–5 percent euhedral garnet in addition to epidote-clinozoisite. Most known occurrences appear to represent epidote-amphibolite-facies conditions.

Within several hundred meters of intrusions, Fairbanks-Chena amphibolite is partly recrystallized to a rock with semi-random amphibole orientations, strongly calcic (An_{75-95}) plagioclase, and commonly trace to 5 percent diopside. More commonly, amphibolite is partly to almost completely retrograded. Such rocks contain 0–15 percent relict plagioclase, 5–35 percent secondary albite, 10–25 percent clinozoisite-epidote, 3–40 percent actinolite, 5–45 percent chlorite, 1–10 percent calcite, 3–10 percent quartz, and 1–5 percent sericite. Relict plagioclase and especially hornblende are the only indications that such rocks were true amphibolites.

The magnetic susceptibility of the unit ranges from low to high, mostly moderate and ranges from 0.0 to 3.3×10^{-3} SI, with an average of 0.18×10^{-3} SI and a median of 0.11×10^{-3} SI. The low values reflect metasedimentary rocks mixed in with the unit. In a few cases, amphibolite bodies could be traced using aeromagnetic highs (Emond and MPX Geophysics, Ltd., 2022). A “metadiorite” from this unit yielded a U-Pb crystallization age of 433 ± 26 Ma (sample 20AJJ039; Kreiner and others, 2025). This unit is correlated with unit P̶zrp (amphibolite in the Chena River sequence) of Smith and others (1994), unit Zfa (amphibolite in the Fairbanks schist) of Newberry and others (1996), and unit MDfca (Fairbanks-Chena amphibolite) of Twelker and others (2025).

MDfco

ORTHOGNEISS OF FAIRBANKS-CHENA ASSEMBLAGE (MISSISSIPPIAN to DEVONIAN)—At least one large (>10 sq km) coherent body and many smaller (0.5–3 sq km) bodies are present in Fairbanks-Chena assemblage rocks, especially in the southwestern SE Chena and west-central NE Chena map areas. Many occurrences are too small to show at map scale, and tiny, unmapped occurrences are moderately common in unit pMfcsg (schist and gneiss). Approximately 15 percent of orthogneiss samples have diorite or quartz diorite compositions, 15 percent have granodiorite or tonalite compositions, and 70 percent have granite compositions. Of the latter, approximately one-fifth contain 5–35 mm alkali feldspar porphyroclasts (“augen”). The unit also includes up to 10 percent interlayered metasedimentary rocks.

Granite orthogneiss is mostly fine- to medium-grained, locally mylonitic or schistose, with a typical grain size of 0.1–4 mm. The rocks are tan, light brown, and gray, and minimally to strongly weathered with varying degrees of chloritic and sericitic alteration. Mineralogy includes 25–35 percent anhedral to subhedral alkali feldspar, commonly twinned and inclusion-rich; 20–35 percent subhedral plagioclase with polysynthetic twinning and minor to major sericite alteration; 35–40 percent subhedral to anhedral dynamically recrystallized quartz; 5–10 percent biotite (variably altered to chlorite); and 2–10 percent muscovite. Biotite and muscovite commonly define the foliation. Accessory minerals variably present include garnet, apatite, zircon, epidote, ilmenite, and titanite.

Granodiorite orthogneiss is similar but contains less alkali feldspar (10–15 percent) with a maximum grain size of 3 mm, and more plagioclase (30–35 percent), biotite (10–15 percent), and hornblende (1–5 percent). Secondary sericite and chlorite are present, but muscovite is absent. Tonalite, diorite, and quartz diorite orthogneiss essentially lack alkali feldspar (0–3 percent) and contain significant hornblende (15–40 percent), 35–55 percent plagioclase, and 2–15 percent epidote, in addition to 1–25 percent biotite. Titanite (0.5–2 percent) and apatite (0.5 percent) are ubiquitous.

Magnetic susceptibility is generally low but variable (0.0 to 38×10^{-3} SI), with an average of 0.35×10^{-3} SI and a median of 0.1×10^{-3} SI; the resulting mean–median disparity is largely due to elevated values in intermediate-composition orthogneiss and the inclusion of metasedimentary rocks. This is mostly due to higher values for intermediate composition (diorite and quartz diorite) orthogneiss and the inclusion of some metasedimentary rocks in the unit. MDfco Fairbanks-Chena orthogneiss described in this report is correlated with unit MDfco (Fairbanks Chena orthogneiss) of

Twelker and others (2025) and with unit Mog (orthogneiss) in the Fairbanks area (Newberry and others, 1996). A sample from the latter yielded a U-Pb crystallization age of 351 ± 2 Ma (Newberry and others, 1998). A small granite orthogneiss body 13 km northeast of West Point (central NE Chena map) yielded a U-Pb crystallization age of 345.8 ± 2.1 Ma (sample 23Z145; Buchanan, Gavel, Barrera, and others, 2025).

pMfccs

CALC-SILICATE GNEISS OF FAIRBANKS-CHENA ASSEMBLAGE (PRE-MISSISSIPPIAN)—Metamorphic calc-silicate rocks are seen sporadically in the Fairbanks-Chena schist and gneiss (pMfcsg) unit and especially in the schist, calc-silicate, and carbonate (pMfcsc) unit. Mappable bodies of calc-silicate gneiss mostly occur as a cluster of lenticular bodies in the west-central part of the NE Chena map, as two lenticular bodies in the east-central part of the NW Chena, and as a larger body (2 sq km) in the eastern SW Chena map (just north of the Salcha River). The known calc-silicate rocks are banded pale green (diopside) to dark green (amphibole) and white (plagioclase + quartz), commonly with some brown patches of garnet ± vesuvianite. Calc-silicate rocks occur as two main mineralogical varieties: a quartz-poor type that makes up roughly two-thirds of occurrences, and a quartz-rich type that comprises about one-third of occurrences. Both types contain diopside or hornblende, but rarely both. Both are recrystallized to calc-silicate granofels or skarn near large granitic bodies. Quartz-poor types contain 2–15 percent quartz, 0–60 percent Ca-rich plagioclase (An_{50-95}), 0–70 percent diopside (or, rarely, hornblende), 0–25 percent calcic garnet, 0–15 percent alkali feldspar, 0–10 percent biotite, 0–15 percent calcite, 0.5–2 percent titanite, 0–1 percent apatite, 0–2 percent sericite (alteration of plagioclase), 0–35 percent epidote-clinozoisite (some is likely alteration of garnet or plagioclase), and 0–1 percent vesuvianite. Skarn is a recrystallized variety with coarser (to 2.5 cm) and more iron-rich (hedenbergite) clinopyroxene, higher (to 50 percent) garnet abundance, and lower plagioclase abundance (near zero). Such rocks also display little or no mineral banding.

Quartz-rich types contain 25–35 percent quartz, 0–30 percent Ca-rich plagioclase (An_{50-80}), 20–35 percent diopside or amphibole, 0–20 percent garnet, 0.5–1 percent titanite, 0–15 percent alkali feldspar, 0–10 percent biotite, 0–2 percent calcite, 0–0.5 percent apatite, and 0–25 percent clinozoisite (in part a replacement of garnet and plagioclase).

Magnetic susceptibility is generally low and ranges from 0.12 to 0.79×10^{-3} SI, with an average of 0.3×10^{-3} SI and a median of 0.24×10^{-3} SI; higher values are present in hornfelsed rocks. This unit is correlated with unit Pzrcs (calc-silicate rocks of the Chena River sequence) of Smith and others (1994) and with unit pMfccs (calc-silicate gneiss) of Twelker and others (2025).

pMfcg

GRAPHITIC ROCKS OF FAIRBANKS-CHENA ASSEMBLAGE (PRE-MISSISSIPPIAN)— Graphitic rocks are a rare variety of Fairbanks-Chena assemblage and are usually not map-scale in extent. A 0.04-sq-km lens is present in the central NW Chena map area. Graphitic Fairbanks-Chena assemblage rocks are likely two-thirds or more schist and one-third or less quartzite. Graphitic quartzite is 85–90 percent quartz, 5–8 percent muscovite, 0–5 percent plagioclase, and 1–2 percent graphite. Graphitic schist contains 5–50 percent anhedral quartz (0.03–2 mm), 10–15 percent subhedral plagioclase (0.1–1.5 mm, some partly altered to albite), 30–55 percent subhedral muscovite (0.05–1.5 mm), 2–15 percent subhedral biotite (0.05–0.5 mm), 3–15 percent subhedral chlorite (0.03–0.2 mm, mostly replacing biotite), 1–2 percent subhedral ilmenite ± rutile ± titanite (0.05–0.2 mm), and 1–5 percent mostly anhedral graphite (0.01–0.05 mm).

Magnetic susceptibility is poorly constrained by the small number of samples, but mostly low and ranges from 0.006 to 0.16 × 10^{-3} SI, with an average of 0.06 × 10^{-3} SI and a median of 0.03 × 10^{-3} SI. This unit is correlated with unit Pzrg (graphitic schist of the Chena River sequence) of Smith and others (1994), with unit CZq (graphitic schist and quartzite) of Athey and others (2022), and with unit pMfcg (Fairbanks-Chena graphitic rocks) of Twelker and others (2025).

pMfcm

MARBLE OF FAIRBANKS-CHENA ASSEMBLAGE (PRE-MISSISSIPPIAN)—Nearly pure to impure marble is sporadically present in the schist and gneiss (pMfcsg) and schist, calc-silicate and carbonate (pMfcsc) units; it also forms mappable bodies in the NW, NE, and SE Chena map areas. Most such bodies are lenticular and small (0.03–0.1 sq km), several bodies are moderate-sized (0.5–2 sq km). About half of this unit is impure marble, with 30–55 percent calcite; most of the rest is marble, with 60–95 percent calcite. About 5 percent of this unit is other rock types, most commonly calc-silicate gneiss or calc-schist.

Impure marble is light gray to light blueish green, and fine to coarse grained (0.1–3.5 mm), some with gneissic banding. In addition to 30–50 percent calcite, impure marble contains 1–15 percent quartz, 0–20 percent diopside, 10–35 percent plagioclase, 0–10 percent clinozoisite, 0–10 percent alkali feldspar, 2–20 percent white mica, 0–12 percent phlogopite, and 0–1 percent titanite. Marble contains 60–95 percent calcite, 0–30 percent quartz, 0–20 percent diopside, 5–15 percent plagioclase, 0–10 percent phlogopite, 0–10 percent white mica, 0–5 percent tremolite, 0–5 percent clinozoisite, and 0.1–0.5 percent apatite.

Magnetic susceptibility is low and ranges from 0.008 to 0.21 × 10^{-3} SI, with a mean and median of 0.08 × 10^{-3} SI. This unit is correlated with unit Pzrm (marble in Chena River sequence) of Smith and others (1994), with unit Zfm (marble in Fairbanks schist) of

Newberry and others (1996), and with unit pMfcm (Fairbanks-Chena marble) of Twelker and others (2025).

pMfcp

PARAGNEISS OF FAIRBANKS-CHENA ASSEMBLAGE (PRE-MISSISSIPPIAN)—Paragneiss is a common rock type in the Fairbanks-Chena assemblage and occurs in many of the units. Areas entirely or almost entirely paragneiss appear restricted to several small (0.4–1.5 sq km) and four large (17–33 sq km) bodies in the northern NW Chena and NE Chena map areas. Paragneiss—especially quartz-rich (65–75 percent quartz) paragneiss—can be easily confused with quartzite; we have employed handheld XRF analyses, commercial major-oxide analyses, and thin-section petrographic analysis to distinguish between these rock types. Conversely, paragneiss with lower quartz contents (45–60 percent quartz) can be confused with orthogneiss. We have employed those same tools to make that distinction. Both types of paragneiss are predominantly black and white or tan to dark gray, weathering gray to dark brown. Grain sizes are typically 0.1–2 mm; gneissic bands are typically 0.5–2 mm wide and dominated by quartz and plagioclase. The two types are of sub-equal abundance.

High-quartz paragneiss contains 65–75 percent anhedral quartz (0.05–2.5 mm), 10–20 percent subhedral plagioclase (0.05–0.8 mm, $An_{20–25}$, slightly altered to sericite), 1–10 percent subhedral biotite (0.2–1.5 mm, well-aligned in foliation, typically with trace to minor chlorite replacement), 2–10 percent subhedral to anhedral white mica (0.02–0.8 mm, aligned parallel to biotite or as partial alteration of plagioclase, 0–5 percent subhedral alkali feldspar (0.05–1 mm, little-altered), 0–1 percent euhedral to subhedral-skeletal garnet (0.03–0.8 mm, slightly to completely replaced by chlorite), 0–8 percent subhedral chlorite (0.03–0.4 mm, mostly aggregates replacing biotite and (or) garnet), and 0–2% anhedral calcite (0.05–0.3 mm, mostly replacing plagioclase). Minerals in trace abundance include ilmenite, hematite, rutile, and tourmaline.

Moderate-quartz paragneiss is like high-quartz paragneiss but contains less quartz (45–60 percent) and more plagioclase (10–30 percent), biotite (5–15 percent), garnet (0.2–4 percent), and ilmenite (0–1 percent). Two unusual types of very low, but uncertain, abundance include those with minor (a) hornblende or (b) staurolite + kyanite.

Magnetic susceptibility of this unit is low and ranges from 0.03 to 0.3×10^{-3} SI, with an average of 0.11×10^{-3} SI and a median of 0.1×10^{-3} SI. This unit correlates with paragneiss in the paragneiss and schist unit of Twelker and others (2025).

pMfcq

QUARTZITE OF FAIRBANKS-CHENA ASSEMBLAGE (PRE-MISSISSIPPIAN)—Quartzite occurs in unit pMfcqp (quartzite and paragneiss) and sporadically in unit pMfcsg (schist and gneiss). Where sufficiently common, it has been mapped as irregular lenses of unit pMfcq. This unit is problematic because fine-grained quartz is difficult to distinguish from fine-grained feldspar in the field. Unit pMfcq was identified in numerous locations in the northeast corner of the SE Chena map, as shown in Werdon and others (2004). Based on our experience with rock identification using handheld XRF while mapping in areas previously identified as quartzite, we suspect that many, if not most, of the areas identified as quartzite on Werdon and others (2004) are not. Lacking quantitative data on the samples, however, we have elected to retain that designation.

Quartzite is gray to pale green and weathers light tan to orange; very fine-grained to medium-grained (0.03–1 mm); weakly foliated; and contains 83–88 percent quartz (anhedral, sometimes parted by thin mica layers), 3–7 percent white mica (some replacing feldspar), 0–5 percent biotite (variably altered to chlorite), 5–10 percent plagioclase (subhedral to anhedral, locally stretched), 0–3 percent chlorite (mostly replacing biotite), 0–1 percent supergene iron oxide, and variably trace amounts of garnet, rutile, and tourmaline.

Magnetic susceptibility is very low to low, ranging from 0.0 to 0.4×10^{-3} SI, with an average of 0.1×10^{-3} SI and a median of 0.08×10^{-3} SI. This unit is correlated with quartzite in the Chena River sequence (Smith and others, 1994) and in the Fairbanks schist (Newberry and others, 1996), in part with unit pMq in the Salcha River-Pogo area (Werdon and others, 2004), and with unit pMfcq of Twelker and others (2025).

pMfcqp

QUARTZITE AND PARAGNEISS OF FAIRBANKS-CHENA ASSEMBLAGE (PRE-MISSISSIPPIAN)—Paragneiss of the Fairbanks-Chena assemblage commonly occurs with schist; locally quartzite and paragneiss occur together without schist. We identified three moderate-sized (18–27 sq km) bodies of such in the western NW Chena, eastern NW Chena, western NE Chena, and easternmost NE Chena map areas. This unit is approximately two-thirds to three-quarters quartz-rich paragneiss; the rest is mostly quartzite with rare schist. The two rock types do not occur together, but rather, occur 100–200 m apart. Commonly the two alternate with each other. Quartzite is as described for unit pMfcq; paragneiss is typically the quartz-rich variety described for unit pMfcp.

Magnetic susceptibility is low to very low, ranging from 0.02 to 0.2×10^{-3} SI, with an average of 0.09×10^{-3} SI and a median of 0.07×10^{-3} SI. This unit has not been described before but probably correlates with unit pMq of Werdon and others (2004).

pMfcs

SCHIST OF FAIRBANKS-CHENA ASSEMBLAGE (PRE-MISSISSIPPIAN)—Schist is a common rock type in the Fairbanks-Chena assemblage, and given its poor resistance to weathering, may be the most abundant rock type in the assemblage. Schist occurs in most units of the Fairbanks-Chena assemblage. Where sufficiently common with little or no other rock types, it defines the unit pMfcs. Six 0.3- to 23-sq-km bodies of schist have been mapped in the northern part of the NW Chena map area. An additional 68-sq-km body straddles the border between the NW and NE Chena maps. A 50-sq-km and two moderate-sized (27 and 8 sq km) bodies are shown in the eastern part of the NE Chena map.

We define schist as containing at least 20 percent sheet silicates with sub-parallel alignment. Schist is distinguished from paragneiss by higher mica abundance (20–80 percent) and a tendency to readily break into thin sheets. Micas typically form continuous sub-millimeter-thick layers. This rock type shows tremendous mineralogical variations; perhaps greater than any other lithology of the Fairbanks-Chena assemblage. For example, quartz content varies from near-zero to 70 percent. Conversely, sheet silicate (biotite + white mica + chlorite) content varies from 22 to 88 percent, with a mean of 47 percent. Within this diverse group we break out three major compositional types: staurolite-bearing, calcareous, and pelitic. Within the last type we recognize three degrees of retrograde overprints: weak, moderate, and strong.

Staurolite-bearing schist is present in several different places in the NW Chena and especially the NE Chena map areas. Nevertheless, this schist probably represents 1–2 percent of Fairbanks-Chena schist. Significantly, staurolite-free schist does not contain chloritoid, the lower-temperature equivalent aluminous silicate mineral. Consequently, staurolite occurrence is due to an unusually high aluminum bulk composition rather than unusual pressure-temperature (P-T) conditions. Calcareous schist accounts for about 3 percent of Fairbanks-Chena assemblage schist; it occurs in the major schist-bearing units and is especially common in the NE and NW Chena map areas.

Typical staurolite-bearing schist contains 10–30 percent mostly anhedral quartz (0.05–1.5 mm), 10–30 percent subhedral plagioclase (0.1–3 mm, some porphyroblastic, An_{18-31}, locally dusted with sericite), 20–50 percent subhedral muscovite (0.5–3 mm), 2–20 percent subhedral biotite (0.1–3.5 mm), 3–20 percent subhedral to euhedral garnet (variably skeletal, 0.2–10 mm), 3–18 percent subhedral to euhedral staurolite (0.1–6 mm, some slightly altered to sericite), 0.5–2 percent subhedral ilmenite (0.05–0.4 mm), 0–7 percent subhedral kyanite (0.2–1 mm, some partly altered to sericite), 0–0.05 percent euhedral tourmaline (0.02–0.3 mm), 0–2 percent secondary chlorite (0.03–0.5 mm, partial replacements of biotite and garnet), 0–3 percent sericite (0.02–0.05 mm, partial replacements of kyanite and plagioclase), and variably trace amounts of rutile.

Retrograded staurolite-bearing schist contains 5–15 percent chlorite, 3–10 percent sericite; less garnet (1–10 percent), biotite (2–10), and staurolite (1–7 percent), and lacks kyanite.

Typical calc-schist contains 5–50 percent anhedral quartz (0.05–1.2 mm, commonly elongated parallel to micas), 3–25 percent anhedral calcite (0.1–3 mm, commonly elongated parallel to micas), 5–35 percent subhedral plagioclase (0.1–0.5 mm, partly altered to sericite), 5–35 percent subhedral muscovite (0.2–2 mm), 5–30 percent subhedral biotite (0.05–1.5 mm), 1–10 percent subhedral clinozoisite (0.05–0.7 mm, strongly aligned with micas), 0.5–1 percent subhedral titanite (0.05–0.15 mm), 0–3 percent subhedral garnet (0.3–2 mm), and 0–10 percent subhedral chlorite (0.1–0.8 mm, apparently primary, not a replacement of biotite).

Roughly one-quarter of Fairbanks-Chena assemblage pelitic schist is weakly retrograded, half is moderately retrograded, and one-quarter is strongly retrograded. Typical weakly retrograded pelitic schist contains 5–65 percent subhedral to anhedral quartz (0.05–2.5 mm), 10–25 percent subhedral plagioclase (0.1–2 mm, commonly porphyroblastic, An_{20-30}, slightly dusted with sericite), 15–55 percent subhedral muscovite (0.05–2 mm), 8–25 percent subhedral biotite (0.05–1.5 mm, some slightly altered to chlorite), 0–15 percent subhedral to euhedral garnet (0.1–10 mm, commonly porphyroblastic), 0.2–1 percent subhedral ilmenite (0.05–0.2 mm), 0.01–3 percent euhedral tourmaline (0.05–0.6 mm), 0–3 percent subhedral chlorite (0.02–0.5 mm, mostly replacing biotite), and trace sericite after plagioclase.

Strongly retrograded Fairbanks-Chena assemblage pelitic schist contains 10–25 percent chlorite, which partly to completely replaces biotite and garnet; plagioclase is mostly to completely replaced by a mix of albite (up to 15 percent), sericite (1–7 percent), clinozoisite (up to 3 percent), and calcite (up to 1 percent). In some cases, the only indication that the rock is Fairbanks-Chena assemblage schist is the presence of skeletal garnet with its distinctive shapes completely pseudomorphed by clots of fine-grained chlorite. Such rocks also typically contain minor to trace biotite as relicts surrounded by chlorite and albite (commonly porphyroblastic).

Moderately retrograded pelitic schist—the most common type—is intermediate between the two extremes, with one-quarter to two-thirds of the biotite replaced by chlorite and garnet slightly chloritized, especially along cracks and at margins. Some or much of the plagioclase in such rocks is retained and identifiable.

Pelitic schist can be partially to almost fully recrystallized, resulting in micas with semi-random orientations and, locally, andalusite and/or sillimanite. Such rocks are described with unit pMfcrg (recrystallized gneiss and schist).

Magnetic susceptibility of Fairbanks–Chena assemblage schist is moderate to very low, ranging from 0.02 to 0.59×10^{-3} SI, with a mean and median of 0.18×10^{-3} SI. The range in values reflects the highly variable mineralogy of these mica-rich rocks. Previous workers have not broken out a schist-rich unit of the Fairbanks-Chena assemblage, so it cannot be directly correlated with previous map units. However, it corresponds to schist present in the Chena River sequence (Smith and others, 1994), in the Fairbanks schist (Newberry and others, 1996), and the Fairbanks-Chena assemblage schist and gneiss (Twelker and others, 2025).

pMfcsg

SCHIST AND GNEISS OF FAIRBANKS-CHENA ASSEMBLAGE (PRE-MISSISSIPPIAN)—This is a composite unit that contains most of the Fairbanks-Chena rock types, although predominantly gneiss and schist. It also accounts for more than half of the Fairbanks-Chena assemblage exposed in the Chena Map area. This unit differs from most other Fairbanks-Chena units in that the two rock types are typically present at a given exposure, commonly interlayered on scales of centimeters to tens of meters. Exposures vary from mostly schist to mostly gneiss, but overall, the unit is likely half to two-thirds gneiss. Paragneiss accounts for about 90 percent of the gneiss; the remaining 10 percent is mostly granitic orthogneiss. Perhaps 5 percent of the unit consists of marble, amphibolite, calc-silicate gneiss, quartzite, quartz veins, and dike rocks, present as bodies too small to map at 1:100,00 scale.

Schist is as described for unit pMfcs (schist) and paragneiss for unit pMfcp (paragneiss).

Magnetic susceptibility of this unit is generally low but variable, ranging from 0.0 to 27 $\times 10^{-3}$ SI, with an average of 0.22×10^{-3} SI and a median of 0.14×10^{-3} SI. This variation reflects the wide range of rock types in the unit and the effects of local contact metamorphism. This unit is correlated with similar rocks in the upper Chena area (Smith and others, 1994), with the Fairbanks schist of Newberry and others (1996), and with unit pMfcsg (schist and gneiss) in the Richardson Mining District (Twelker and others, 2025). Schist presumably represents more clay-rich protoliths, and paragneiss represents more arkosic protoliths. The age is constrained by the apparent intrusion of Mississippian granites, now orthogneiss (unit MDfco).

pMfcsc

SCHIST, CALC-SILICATE, AND CARBONATE ROCKS OF FAIRBANKS-CHENA ASSEMBLAGE (PRE-MISSISSIPPIAN)—This is a mixed unit, like ‘schist and gneiss’ but with abundant calcareous components: marble, impure marble, calc-silicate gneiss, calc-schist, and skarn mixed with pelitic schist, paragneiss, and minor amphibolite. Multiple, interlayered lithologies can be present at a given occurrence with banding on a scale of decimeters to meters. These include marble-schist, marble-amphibolite, marble-calc-silicate gneiss, and calc-silicate gneiss-schist interlayered rocks. This unit appears to be mostly confined to the NE Chena map area, where it occurs as 9 small (1.5–3 sq km) to moderate-sized (8–22 sq km) bodies.

The proportions of component lithologies vary, but overall, about 10 percent is marble or impure marble, 50 percent is calc-silicate gneiss + calc-schist, and the remainder is mostly pelitic schist with minor amounts of paragneiss, orthogneiss, and amphibolite. Rock types in this unit have been described with the descriptions of amphibolite (MDfca), calc-silicate gneiss (pMfccs), marble (pMfcm), paragneiss (pMfcp), and schist (pMfcs). Magnetic susceptibility of this unit is generally low, but variable (0.02–0.7 x 10^{-3} SI, with an average of 0.19 x 10^{-3} SI and a median of 0.18 x 10^{-3} SI). This variation reflects the variety of lithologies in the unit. Previous workers have not broken out a unit of the Fairbanks-Chena assemblage with the particular lithologic combination seen in pMfcsc; it cannot be directly correlated with previous map units.

pMfcrg

RECRYSTALLIZED GNEISS AND SCHIST OF FAIRBANKS-CHENA ASSEMBLAGE (PRE-MISSISSIPPIAN)—Schist and gneiss are partly to strongly recrystallized where present within 200–300 meters of granitic contacts or in roof pendants above granitic bodies. Locally occurring rocks are not broken out in the Chena map area but small roof pendants that consist entirely of recrystallized rocks are identified. Large bodies of sillimanite-bearing (and locally cordierite-bearing) gneiss were mapped by Werdon and others (2004) in the vicinity of (and above?) Harper suite batholiths in the northeast and southwest parts of the SE Chena map area. In addition, a small body of recrystallized gneiss is present adjacent to the low-angle contact with Lake George assemblage recrystallized gneiss, 4.5 km south of West Point (central NE Chena map). These large bodies of recrystallized gneiss and schist contain up to 20 percent other rock types, including marble, calc-silicate rocks, amphibolite, quartzite, orthogneiss, granitic rocks, and rocks lacking evidence for recrystallization.

Rocks of this unit display considerable textural and mineralogical variations due to protolith variations. Recrystallization is typically seen as a second generation of micas oriented at high angle to mineralogical banding; these commonly differ from foliation-parallel grains in size. At a minimum about one-fifth of the micas display such characteristics; at the other extreme micas are up to 6 mm and possess random orientations. The latter texture (granofels) is particularly characteristic of rocks in small roof pendants. Similar grain size enlargement can occur in other minerals: quartz (up to 5 mm), plagioclase (up to 3 mm), and muscovite (up to 3.5 mm). Sillimanite typically occurs as bundles of 0.1–0.3 mm fibers, some oriented sub-parallel to mica-defined foliation, some at high angle to it. Relict kyanite is locally present, partly altered to white mica. Retrograde alteration of aluminosilicates (including cordierite) to sericite and biotite to chlorite is common in samples near granite contacts.

Mineralogy of these rocks includes 5–65 percent quartz, 5–40 percent plagioclase, 3–55 percent muscovite, 3–40 percent biotite, 0.5–1 percent ilmenite, 0–20 percent chlorite, 0–45 percent sericite, 0–15 percent garnet, 0–15 percent cordierite, and 0–15 percent sillimanite. Minerals locally include andalusite (to 10 percent), relict kyanite (to 1 percent), tourmaline (to 0.5 percent), and staurolite (to 3 percent).

Magnetic susceptibility of this unit is generally low but variable, ranging from 0.01 to 1.7×10^{-3} SI, with a mean of 0.13×10^{-3} SI and a median of 0.11×10^{-3} SI. This variation reflects the wide variety of lithologies in the unit and the variable degree of recrystallization and retrograde alteration. The age is based on other Fairbanks-Chena assemblage metasedimentary rocks. This unit is partially correlated with unit pMp of Werdon and others (2004).

Lake George Assemblage

The amphibolite-facies Lake George assemblage is interpreted to occupy the lowest structural level in the project area. The assemblage is composed of augen gneiss, orthogneiss, amphibolite, paragneiss, schist, and quartz schist, with minor quartzite and rare marble. The metasedimentary lithologies may be the metamorphosed equivalents of the Neoproterozoic to Devonian passive-margin strata of the Selwyn Basin, which were deposited prior to the intrusion of Mississippian-Devonian granitic plutons. Orthogneiss and amphibolite mostly occur as layers concordant with foliation in the metasedimentary rocks. The rocks were metamorphosed to upper amphibolite-facies (Newberry and Twelker, 2021) in the Early Cretaceous (Wildland, 2022) prior to rapidly cooling through the $^{40}Ar/^{39}Ar$ closure temperatures of multiple chronometers in the mid-Cretaceous (Pavlis and others, 1993; Dusel-Bacon and others, 2002; Jones and Benowitz, 2020; Naibert and others, 2020).

MDla

AMPHIBOLITE OF THE LAKE GEORGE ASSEMBLAGE (EARLY MISSISSIPPIAN to LATE DEVONIAN)—Mostly hornblende amphibolite with 5 percent hornblende diorite to hornblende quartz diorite orthogneiss; typically present as thin, 0.5–2-km-long lenses in (or adjacent to) unit MDlo (orthogneiss). The rock is dark green to gray, commonly weathers to brown, and is fine- to medium-grained; it is dominantly gneissic-textured. The predominant rock type is hornblende amphibolite (some partially retrograded to greenschist facies) with a grain size of 0.1–2 mm. Typical mineralogy includes 45–65 percent hornblende (0.1–2 mm, subhedral, some with relict actinolite cores or late rims, some alteration to chlorite), 15–35 percent calcic plagioclase (0.05–1 mm subhedral grains, partly altered to sericite or clinozoisite, mostly An_{40-85}), 0–8 percent biotite (0.05–0.5 mm, typically with some alteration to chlorite), 0.3–5 percent chlorite (0.02–0.3 mm, partial replacement of hornblende and especially biotite), 0–2 percent garnet (0.1–1 mm, subhedral to euhedral), 0–10 percent diopside (0.05–0.8 mm, subhedral grains partly altered to actinolite), 0–4 percent clinozoisite-epidote (0.03–0.5 mm, subhedral to anhedral grains and clusters that mostly replace plagioclase), 0.5–2 percent apatite (0.05–0.3 mm, subhedral grains), and 0.5–5 percent ilmenite + titanite + rutile. Quartz, magnetite, and pyrrhotite are variably present in small amounts. Hornblende quartz diorite orthogneiss is similar, but contains 5–10 percent quartz, less plagioclase, and lacks diopside. Strongly retrograded samples contain up to 25 percent clinozoisite-epidote, 15 percent chlorite, and abundant secondary albite and actinolite.

Magnetic susceptibility is mostly moderate, ranging from 0.40 to 1.8×10^{-3} SI, with an average of 0.8×10^{-3} SI and a median of 0.6×10^{-3} SI. Correlated with Lake George assemblage amphibolite of Twelker and others (2021), Wypych and others (2021), and Twelker and others (2025), and with unit pMa in the Alaska Highway corridor (Solie and others, 2019). A U-Pb zircon age of 351.5 ± 4.3 Ma from correlative amphibolite was collected in the northeast Tanacross Quadrangle (sample 18AW074; Wypych and others, 2020).

MDlo

ORTHOGNEISS OF THE LAKE GEORGE ASSEMBLAGE (EARLY MISSISSIPPIAN TO LATE DEVONIAN)— A widely distributed unit in the Lake George assemblage that in the Chena map area contains approximately 5 percent tonalite and granodiorite orthogneiss and 95 percent granite orthogneiss. Of the latter, approximately 15 percent contain 5–30 mm alkali feldspar augen.

Granite orthogneiss is mostly fine- to medium-grained and is locally mylonitic or schistose, with a typical grain size of 0.1–3 mm; rare alkali-feldspar augen are up to 4 cm. The rocks are tan, light brown, and gray, minimally to moderately weathered, and have experienced varying degrees of chloritic and sericitic alteration. Their mineralogy includes 25–35 percent alkali feldspar (mostly 0.2–3 mm, anhedral to subhedral grains, commonly twinned and inclusion-rich); 20–35 percent plagioclase (0.1–2 mm, subhedral grains with polysynthetic twinning and minor to significant sericite alteration); 25–35 percent quartz (0.1–3 mm, subhedral to anhedral dynamically recrystallized grains with undulose extinction); 1–10 percent biotite (0.05–1 mm, variably altered to chlorite); 0–14 percent white mica (0.02–2 mm, subhedral grains, some a partial replacement of plagioclase); 0–2 percent chlorite (partial replacement of biotite and partial alteration of hornblende and garnet); 0–0.5 percent garnet (0.1–0.5 mm, subhedral to euhedral grains, some partly altered to chlorite). Biotite and muscovite commonly define the foliation. Accessory minerals locally present include magnetite, apatite, zircon, epidote, ilmenite, allanite, and titanite.

Granodiorite and tonalite orthogneiss are similar but contain less alkali feldspar (6–15 percent), with a maximum grain size of 3 mm, and more plagioclase (30–45 percent) and variable hornblende (0–5 percent). Secondary sericite and chlorite are present, but muscovite is absent.

The unit generally has low magnetic susceptibility, ranging from 0.015 to 2×10^{-3} SI, with an average of 0.13×10^{-3} SI and a median of 0.1×10^{-3} SI. A chloritized granite orthogneiss near the southwestern border of the SE Chena map yielded a U-Pb zircon age of 361.7 ± 2.7 Ma (22RN537; Buchanan, Gavel, Wildland, and others, 2025). A Lake George granite orthogneiss from the western Tanacross Quadrangle yielded a U-Pb zircon crystallization age of 359.6 ± 1.3 Ma (sample 21SPR150; Gavel and others, 2023). This unit correlates to the Lake George orthogneiss of Twelker and others (2021), Wypych and others (2021), Naibert and others (2024), and Twelker and others (2025).

pMlms

METASEDIMENTARY ROCKS OF THE LAKE GEORGE ASSEMBLAGE (PRE-MISSISSIPPIAN)—A composite unit; it comprises approximately 10 percent orthogneiss, and 90 percent metasedimentary rocks. The latter includes about half schist, half paragneiss, and less than one percent each of quartzite and calc-silicate rocks. This unit is uncommon in the map area and is mostly present as 1- to 10-sq-km bodies in the northeast corner of the SW Chena map.

Paragneiss is predominantly black and white or tan to dark gray, weathering gray to dark brown. Grain sizes are typically 0.1–2 mm. Gneissic bands are typically 0.5–2 mm wide, dominated by quartz and feldspar; biotite occurs in bands that visibly define the gneissic texture. Minerals present include: 40–65 percent quartz (0.1–2 mm, commonly anhedral grains with undulatory extinction and irregular grain boundaries), 15–30 percent plagioclase (0.2–1.5 mm, commonly twinned, forms bands, variably altered to sericite), 0–10 percent alkali feldspar (0.2–0.6 mm, subhedral grains, little-altered), 5–10 percent biotite (0.2–0.7 mm, typically with trace to major chlorite replacement); 1–10 percent muscovite (0.1–1 mm), 0–5 percent garnet (0.05–1.5 mm subhedral grains, some partly replaced by chlorite), 0.5–2 percent sericite (slightly to strongly replaces plagioclase and to a smaller extent, alkali feldspar), 0–3 percent chlorite (trace to major replacement of biotite); and minor ilmenite, titanite, and apatite.

Schist contains more mica than paragneiss; the micas typically form continuous sub-millimeter-thick layers. Grains are typically 0.1–2 mm. The schist typically contains 20–55 percent quartz (0.1–1.5 mm, typically with undulatory extinction and irregular grain boundaries), 5–35 percent plagioclase (0.1–2 mm, commonly twinned, forms bands, partly replaced by sericite and [or] clay), 0–7 percent alkali feldspar (0.1–1 mm, some twinned, little-altered), 5–60 percent muscovite (0.1–2 mm, subhedral to euhedral), 5–30 percent biotite (0.1–1 mm, slightly to moderately replaced by chlorite); 0–5 percent garnet (0.05–2 mm, subhedral to euhedral), 0.2–5 percent sericite (partial alteration of plagioclase), 0.3–5 percent chlorite (slight to significant alteration of biotite), and 0–0.5 percent tourmaline (0.05–0.5 mm, euhedral grains). Other minerals, variably present in small amounts include ilmenite, rutile, apatite, and zircon. Quartz schist is similar and relatively rare; it contains more quartz (60–70 percent) and less total feldspar (5–15 percent).

Quartzite is gray to pale green and weathers light tan to orange; very fine- to fine-grained (0.05–0.5 mm); weakly foliated; and is composed of 80–95 percent quartz (anhedral, sometimes parted by thin mica layers), 1–10 percent muscovite (fine-grained, often as single-crystal layers); 0–5 percent biotite (slightly to partly altered to chlorite), 5–10 percent plagioclase (anhedral, usually untwinned grains, locally stretched, partly altered to sericite), 0–1 percent garnet (subhedral to euhedral grains, some slightly chloritized), 0.3–1.5 percent chlorite (variably replaces biotite and garnet), and variably trace calcite, alkali feldspar, and pyrite.

Calc-silicate rocks possess distinct mineralogical banding and are dominated by diopside, epidote, plagioclase, garnet, and quartz.

Unit pMlms has generally low but variable magnetic susceptibility, ranging from 0.04 to 2.3 × 10^{-3} SI, with an average of 0.28 × 10^{-3} SI and a median of 0.18 × 10^{-3} SI. The presence of orthogneiss within the metasediments suggests that sediment deposition occurred prior to the Early Mississippian minimum age of unit MDlo. A detrital zircon sample southeast of the project area along the Taylor Highway (south of Taylor Mountain) yields a youngest U–Pb age population of 515–555 Ma (sample 16YTT021; Jones and O'Sullivan, 2020), indicating that the protolith sediment is Cambrian or younger. The composite unit likely comprises the metamorphic equivalents of at least parts of the Neoproterozoic through Devonian Selwyn Basin stratigraphy. This unit is correlated with Lake George metasedimentary rocks (pMlms) of Wypych and others (2021), Naibert and others (2024), and Twelker and others (2025).

pMlp

PARAGNEISS OF THE LAKE GEORGE ASSEMBLAGE (PRE-MISSISSIPPIAN)—Unit is about 20 percent orthogneiss, and 80 percent metasedimentary rocks, which are predominantly paragneiss, with lesser schist and rare calc-silicate rocks and thin marble bands. This unit contains the same lithologies as unit pMlms, but the metasedimentary rocks are dominantly paragneiss.

Magnetic susceptibility of this unit is generally low but variable, ranging from 0.01 to 7.4 × 10^{-3} SI, with an average of 0.3 × 10^{-3} SI and a median of 0.12 × 10^{-3} SI. This is due in part to the variety of rock types present; additionally, calc-silicate rocks in this unit show considerable variation. Orthogneiss bodies within the unit suggest sediment deposition occurred prior to the Early Mississippian minimum age of MDlo. An anthophyllite granofels sample of uncertain protolith in this unit (sample 22Z237) yielded a U-Pb crystallization age of 365 ± 2 Ma (Buchanan, Gavel, Wildland, and others, 2025). This unit is correlated with the Scottie Creek Formation in western Yukon (Yukon Geological Survey, 2019) and Lake George paragneiss (pMlp) of Naibert and others (2024) and Twelker and others (2025).

pMlrp

RECRYSTALLIZED PARAGNEISS OF THE LAKE GEORGE ASSEMBLAGE (PRE-MISSISSIPPIAN)—A unit that occurs in three major areas of the Chena map: the Salcha River gneiss dome (Dusel-Bacon and others, 2002) in the southeast corner of the SW Chena map, another likely gneiss dome (Dusel-Bacon and others, 2003) in the West Point area (central NE Chena map), and a 100 sq km area south of (and above?) the Goodpaster Batholith in the southeastern SE Chena map. The first areas contain sillimanite-bearing rocks and are thought to be structurally beneath the Fairbanks-Chena assemblage rocks based on industry drilling data in the Richardson area (Graham, 2002). The last area contains andalusite ± sillimanite-bearing rocks and may represent a regional-scale contact metamorphic zone.

Rocks of this unit display considerable textural and mineralogical variation, the latter due to protolith (paragneiss versus schist). Recrystallization is typically expressed as a second generation of micas oriented at high angles to mineralogical banding; these grains commonly differ in size from foliation-parallel micas. At a minimum, about one-fifth of the micas display such characteristics; at the other extreme, micas are up to 3 mm and possess random orientations. The latter texture (granofels) is particularly characteristic of the andalusite-bearing rocks south of the Goodpaster batholith. Other minerals in these rocks are also enlarged, for example, quartz (up to 3.5 mm), plagioclase (up to 2.5 mm), alkali feldspar (up to 3 mm), and muscovite (up to 1.5 mm). Andalusite porphyroblasts are up to 5 mm, and sillimanite can occur as prisms up to 1.5 mm long. In contrast, recrystallized paragneiss from the Salcha River and West Point gneiss domes does not exhibit as much grain size enlargement (grains are mostly less than 2 mm) and typically half or less of the micas display re-orientation.

The rock type at the gneiss domes most likely underwent recrystallization during a relatively high-temperature, moderate-pressure, fluid-influx event. Based on the variable presence of either muscovite or alkali feldspar with sillimanite, at least some recrystallization is due to the reaction quartz + muscovite = sillimanite + orthoclase. Not all rocks in the gneiss domes are sillimanite-bearing (orthogneiss bodies, for example, lack it), but perhaps as much as two-thirds are.

Recrystallized Lake George assemblage paragneiss is predominantly black and white, or tan to dark gray, and weathers to gray to dark brown. Gneissic bands are typically 0.5–2 mm wide, dominated by quartz and feldspar; biotite occurs in bands, but grains display some semi-random orientations. Minerals present include: 40–70 percent quartz, 5–25 percent plagioclase, 0–10 percent alkali feldspar, 2–20 percent biotite (typically with trace to major chlorite replacement), 0–10 percent sillimanite (mostly bundles of 0.05–0.15 mm fibers, with rare prismatic grains), 0–10 percent muscovite, 0–4 percent garnet, 0–10 percent sericite (partly replaces plagioclase and partly to nearly completely replaces sillimanite), 0–10 percent chlorite (variably replaces biotite), and 0–1 percent ilmenite. The major mineralogical difference between the ‘gneiss-dome’ type and the batholith-associated type is the common occurrence of andalusite (0–10 percent) in the latter.

Schist locally occurs in this unit, especially in the ‘gneiss dome’ type. The micas commonly display partial recrystallization with semi-random as well as well-aligned grains. Due to partial recrystallization, this schist commonly does not break into thin sheets; however, the micas typically form continuous sub-millimeter-thick layers. Grain size is typically 0.05–1 mm. This partly recrystallized schist typically contains 30–55 percent quartz, 5–30 percent plagioclase (An_{25-45}), 1–7 percent alkali feldspar, 0–10 percent muscovite, 0–15 percent sillimanite, 15–35 percent biotite (slightly replaced by chlorite), 0–5 percent garnet, 0.5–10 percent sericite, 0.3–2 percent chlorite (as slight to significant alteration of biotite), and 0.4–1 percent ilmenite. In several cases, sillimanite replaces muscovite or muscovite is absent altogether, suggesting that sillimanite commonly forms from muscovite breakdown in these rocks. The sillimanite, in turn, is slightly to strongly replaced by sericite, reflecting the presence of lower-temperature fluids.

This unit has low magnetic susceptibility, ranging from 0.0 to 0.7 × 10^{-3} SI, with a mean of 0.13 × 10^{-3} SI and a median of 0.12 × 10^{-3} SI. Correlated with recrystallized Lake George paragneiss in the Richardson area (Twelker and others, 2025) and with the Scottie Creek Formation in western Yukon (Yukon Geological Survey, 2019).

pMlmpg MIGMATITIC PARAGNEISS OF THE LAKE GEORGE ASSEMBLAGE (PRE-MISSISSIPPIAN)— Recrystallized paragneiss (unit pMlrp) locally exhibits variably developed migmatitic texture. Two small (2–3 sq km) bodies are identified in the Salcha River gneiss dome (in SW Chena map); others are likely present. In this mixed rock, biotite-feldspar-quartz paragneiss melanosomes form irregular to rounded bodies, typically 1–20 cm in diameter. The melanosome is interlayered with recrystallized leucocratic sillimanite-bearing paragneiss lenses or locally surrounded by an interconnected network of unfoliated, equigranular, fine-grained leucosome composed of quartz, alkali feldspar, plagioclase, and several percent biotite.

Magnetic susceptibility is uniformly low, ranging from 0.02 to 0.25 × 10^{-3} SI, with an average of 0.13 × 10^{-3} SI and a median of 0.14 × 10^{-3} SI. This unit is correlated with migmatitic Lake George paragneiss in the Richardson area (Twelker and others, 2025).

MZlu LAKE GEORGE ASSEMBLAGE, UNDIVIDED (MISSISSIPPIAN to PROTEROZOIC)—This unit is mapped in areas where Lake George assemblage rocks are suspected based on nearby occurrences, but rock exposures are not known, typically due to extensive loess, aeolian sand, or soil cover. Any or all of the various Lake George lithologies could be present at depth in these areas.

ACKNOWLEDGMENTS

Many individuals and organizations assisted us with this project. Thanks to Northern Star Resources Ltd. geologists Paul Hohbach, Karl Sharp, Mike Murenbeeld, Tanya Nayda and others who shared their knowledge, maps, and samples from the Pogo Mine area. Resolution Minerals Ltd. and Christine Lawley shared prior geologic mapping and geophysical models that helped us validate our geologic interpretations in the eastern Pogo trend; thanks also to Kyle Negri and Millrock Resources Inc. for their part in this. Thanks to Peter Franz of Metallogeny Inc. for sharing his knowledge of the Paldo Creek area, as well as Tectonic Metals Inc. and Peter Kleespies for their cooperation in the Tibbs area.

We are grateful for conversations and collaboration with U.S. Geological Survey staff, including Doug Kreiner, Erin Todd, Jamey Jones, and Jonathan Caine. Jacob Murchek's merged aeromagnetic grid was much appreciated during our field mapping.

Thanks to the Arizona LaserChron Center and staff for their assistance with the U-Pb geochronology supporting many of the map unit assignments.

Nathan Graham and the University of Alaska Advanced Instrumentation Laboratory were instrumental (so to speak) in helping us collect mineral compositional data. We thank Florian Hofmann and the University of Alaska Geochronology for their help in generating and interpreting $^{40}Ar/^{39}Ar$ data.

We thank Tim Hammond and Nicole Swensgard of the U.S. Bureau of Land Management Eastern Interior Field Office for assisting us through the permitting process to map in the Steese National Conservation Area. Thanks to Alaska State Parks for their cooperation with our mapping in the Chena River State Recreation Area. Chena Hot Springs Resort and staff went above and beyond to provide us with a great base of operations. We are especially grateful to Keith Warren and Aurora Aviation Services. Keith's safe flying, flawless maintenance, and level-headed demeanor gave us confidence during difficult times.

This project was jointly funded by the State of Alaska capital funds and the U.S. Geological Survey Earth Mapping Resources Initiative (Earth MRI) through cooperative agreement G23AC00372. The views and conclusions contained in this document are those of the authors and should not be interpreted as representing the opinions or policies of the U.S. Geological Survey. Mention of trade names or commercial products does not constitute their endorsement by the U.S. Geological Survey.

REFERENCES

Aleinikoff, J.N., Dusel-Bacon, Cynthia, and Foster, H.L., 1986, Geochronology of augen gneiss and related rocks, Yukon-Tanana terrane, east-central Alaska: Geological Society of America Bulletin, v. 97, p. 626–637.

Athey, J.E., Freeman, L.K., Newberry, R.J., Werdon, M.B., Szumigala, D.J., and Lessard, R.R., 2022, Bedrock geologic map of the northern Fairbanks mining district, Circle Quadrangle, Alaska: Alaska Division of Geological & Geophysical Surveys Preliminary Interpretive Report 2022-2, 24 p., 1 sheet, scale 1:50,000. https://doi.org/10.14509/30891

Athey, J.E., Werdon, M.B., Szumigala, D.J., Newberry, R.J., and Johnson, M.R., 2002, Major-oxide, minor-oxide, trace-element, and geochemical data from the rocks collected in the Big Delta Quadrangle, Alaska in 2001: Alaska Division of Geological & Geophysical Surveys Raw Data File 2002-3, 18 p., 2 sheets, scale 1:150,000. https://doi.org/10.14509/2857

Buchanan, J.W., Barrera, M.L., Gavel, M.M., Truskowski, C.M., Wildland, A.D., Moshrefzadeh, J.A., and Regan, S.P., 2026, LA-ICP-MS uranium lead detrital zircon data from metamorphic and sedimentary rocks from the Yukon-Tanana Upland, Alaska: Alaska Division of Geological & Geophysical Surveys Raw Data File 2026-13, 5 p. https://doi.org/10.14509/32080

Buchanan, J.W., Barrera, M.L., Moshrefzadeh, J.A., Truskowski, C.M., and Newberry, R.J., 2025, LA-ICP-MS uranium-lead zircon data from samples in the Chena and Steese project areas:

Alaska Division of Geological & Geophysical Surveys Raw Data File 2025-25, 4 p. https://doi.org/10.14509/31731

Buchanan, J.W., Barrera, M.L., and Newberry, R.J., 2026, LA-ICP-MS uranium-lead zircon data from igneous rocks collected during the 2025 field season from the Steese-White Mountains and Chena project areas, Yukon-Tanana Upland, Alaska: Alaska Division of Geological & Geophysical Surveys Raw Data File 2026-11, 4 p. https://doi.org/10.14509/32064

Buchanan, J.W., Gavel, M.M., Barrera, M.L., Regan, S.P., and Newberry, R.J., 2025, LA-ICP-MS uranium lead geochronologic data of zircon from igneous and meta-igneous rocks in the Chena project area, Circle, Big Delta, and Eagle quadrangles, Alaska: Alaska Division of Geological & Geophysical Surveys Raw Data File 2025-14, 4 p. https://doi.org/10.14509/31553

Buchanan, J.W., Gavel, M.M., Wildland, A.D., and Newberry, R.J., 2025, LA-ICP-MS uranium lead geochronologic data of zircon from igneous and meta-igneous rocks in the Mount Harper project area, Eagle, Tanacross, Mount Hayes, and Big Delta quadrangles, Alaska: Alaska Division of Geological & Geophysical Surveys Raw Data File 2025-4, 5 p. https://doi.org/10.14509/31552

Buchanan, J.W., Wypych, Alicja, Barrera, M.L., Biegel, J.M., Gavel, M.M., Harvey, D.A., Ketcham, R.A., Muller, I.P., Naibert, T.J., Newberry, R.J., Regan, S.P., Szumigala, D.J., Twelker, Evan, and Wildland, A.D., 2025, Geochemical data from samples collected in 2023 for the Chena and Mount Harper projects, Big Delta, Circle, Fairbanks, and Eagle quadrangles, Alaska: Alaska Division of Geological & Geophysical Surveys Raw Data File 2024-2, 5 p. https://doi.org/10.14509/31123

Bucher, Kurt, and Grapes, Rodney, 2011, Petrogenesis of Metamorphic Rocks, 8th Edition: Springer, New York, 428 p.

Burns, L.E., Graham, G.R.C., Barefoot, J.D., Woods, Rebecca-Ellen, Dighem, and WGM, Inc., 2020, Richardson electromagnetic and magnetic airborne geophysical survey data compilation: Alaska Division of Geological & Geophysical Surveys Geophysical Report 2019-22, 12 p. https://doi.org/10.14509/30263

Day, W.C., Aleinikoff, J.N., Roberts, Paul, Smith, Moira, Gamble, B.M., Henning, M.W., Gough, L.P., and Morath, L.C., 2003, Geologic map of the Big Delta B-2 Quadrangle, east-central Alaska: U.S. Geological Survey Geologic Investigations Series Map 2788, 1 sheet, scale 1:63,360.

Day, W.C., O'Neill, J.M., Aleinikoff, J.N., Green, G.N., Saltus, R.W., and Gough, L.P., 2007, Geologic map of the Big Delta B-1 Quadrangle, east-central Alaska: U.S. Geological Survey Scientific Investigations Map 2975, 1 sheet, scale 1:63,360.

Dilworth, K.M., 2003, Geological setting, nature and evolution of reduced intrusions and gold-bearing quartz veins of the 4021 prospect, Goodpaster district, east-central Alaska: University of British Columbia, M.S. thesis, 192 p.

Dusel-Bacon, Cynthia, and Harris, A.G., 2003, New occurrences of late Paleozoic and Triassic fossils from the Seventymile and Yukon-Tanana Terranes, east-central Alaska, with comments on previously published occurrences in the same area: U.S. Geological Survey Professional Paper 1678, p. 5–30.

Dusel-Bacon, Cynthia, Holm-Denoma, C.S., Jones, J.V. III, Aleinikoff, J.N., and Mortensen, J.K., 2017, Detrital zircon geochronology of quartzose metasedimentary rocks from parautochthonous North America, east-central Alaska: Lithosphere, v. 9, no. 6, p. 927–952. https://doi.org/10.1130/L672.1

Dusel-Bacon, Cynthia, Hopkins, M.J., Mortensen, J.K., Dashevsky, S.S., Bressler, J.R., and Day, W.C., 2006, Paleozoic tectonic and metallogenic evolution of the pericratonic rocks of east-central Alaska and adjacent Yukon Territory: Geological Association of Canada Special Paper 45, p. 25–74.

Dusel-Bacon, Cynthia, Lanphere, M.A., Sharp, W.D., Layer, P.W., and Hansen, V.L., 2002, Mesozoic thermal history and timing of structural events for the Yukon-Tanana Upland, east-central Alaska: Canadian Journal of Earth Sciences, v. 39, p. 1013–1051. https://doi.org/10.1139/e02-018

Dusel-Bacon, Cynthia, Wooden, J.L., and Layer, P.W., 2003, A Cretaceous ion-microprobe U-Pb zircon age for the West Point orthogneiss: U.S. Geological Survey Professional Paper 1678, p. 41–60.

Emond, A.M., and MPX Geophysics Ltd., 2022, Tanana River and Big Delta airborne magnetic and radiometric survey: Alaska Division of Geological & Geophysical Surveys Geophysical Report 2022-1, 4 p. https://doi.org/10.14509/30899

Foster, H.L., Keith, T.E.C., and Menzie, W.D., 1994, Geology of the Yukon-Tanana area of east-central Alaska: Geological Society of America, The Geology of North America, v. G-1, p. 205–240.

Foster, H.L., Laird, Jo, Keith, T.E.C., Cushing, G.W., and Menzie, W.D., 1983, Preliminary geologic map of the Circle Quadrangle, Alaska: U.S. Geological Survey Open-File Report 83-170-A, 30 p., 1 sheet, scale 1:250,000.

Gavel, M.M., Regan, S.P., Holland, Mark, Wildland, A.D., Wypych, Alicja, Naibert, T.J., and Twelker, Evan, 2023, U-Pb zircon geochronology of bedrock samples collected in the Eagle and Tanacross quadrangles, eastern Alaska: Alaska Division of Geological & Geophysical Surveys Preliminary Interpretive Report 2023-2, 38 p. https://doi.org/10.14509/31013

Gavel, M.M., Wypych, Alicja, Naibert, T.J., Twelker, Evan, Newberry, R.J., Barrera, M.L., Szumigala, D.J., Truskowski, C.M., Muller, I.P., Fessenden, S.N., Blackwell, N.J., Harvey, D.A., and Wildland, A.D., 2025, Bedrock geologic map of the Mount Harper-Middle Fork area, Eagle Quadrangle, Alaska: Alaska Division of Geological & Geophysical Surveys Preliminary Interpretive Report 2025-2D, 1 sheet, scale 1:100,000. https://doi.org/10.14509/31652

Graham, G.E., 2002, Geology and gold mineralization of the Richardson district, east-central Alaska: University of Alaska Fairbanks, M.S. thesis, 150 p.

Hart, C.J.R., Goldfarb, R.J., Lewis, L.L., and Mair, J.L., 2004, The Northern Cordilleran mid-Cretaceous plutonic province: Resource Geology, v. 54, no. 3, p. 253–280.

Hendricks, M.D., Macpherson, A.E., Athey, J.E., Wyatt, W.C., Montayne, Simone, Buchanan, J.W., Rivera, P.G., and Steinleitner, A.M., 2024, AK GeMS data dictionary: Alaska Division of Geological & Geophysical Surveys Miscellaneous Publication 170 v. 2, 13 p. https://doi.org/10.14509/31172

Holm-Denoma, C.S., Pianowski, L.S., and Kreiner, D.C., 2022, U-Pb zircon data for igneous units related to mineralization in the eastern Yukon-Tanana upland, eastern Alaska: U.S. Geological Survey data release. https://doi.org/10.5066/P9RANVXY

Jones, J.V. III, and Benowitz, J.A., 2020, $^{40}Ar/^{39}Ar$ isotopic data and ages for rocks from the Yukon-Tanana Upland of eastern Alaska and the northern Aleutian Range of south-central Alaska: U.S. Geological Survey Data Release. https://doi.org/10.5066/P96762V3

Jones, J.V. III, and O'Sullivan, Paul, 2020, U-Pb isotopic data and ages of zircon, titanite, and detrital zircon from rocks from the Yukon-Tanana Upland, Alaska: U.S. Geological Survey Data Release. https://doi.org/10.5066/P9WWV93S

Kreiner, D.C., Holm-Denoma, C.S., Pianowski, L.S., and O'Sullivan, P.B., 2025, U-Pb zircon data for igneous and metaigneous rocks of interior and southwest Alaska: U.S. Geological Survey data release. https://doi.org/10.5066/P1MUQSJA

Lessard, R.R., 2006, Geology of the Caribou Creek area, Big Delta Quadrangle, east-central Alaska: University of Alaska Fairbanks, M.S. thesis, 267 p.

Meschede, Martin, 1986, A method of discrimination between different types of mid-ocean ridge basalts and continental tholeiites with the Nb-Zr-Y diagram: Chemical Geology, v. 56, p. 207–218.

Moshrefzadeh, J.A., Acosta, M.D., Barrera, M.L., Buchanan, J.W., Naibert, T.J., Newberry, R.J., Norwood, L.P., Regan, S.P., Szumigala, D.J., and Twelker, Evan, 2025, Geochemical data from samples collected in 2024 for the Chena and Steese projects, Big Delta, Circle, Fairbanks, and Livengood quadrangles, Alaska: Alaska Division of Geological & Geophysical Surveys Raw Data File 2025-17, 3 p. https://doi.org/10.14509/31692

Moshrefzadeh, J.A., and Newberry, R.J., 2025, Electron probe microanalyzer data collected on samples from the Chena and Steese projects, Yukon-Tanana Uplands, Alaska: Alaska Division of Geological & Geophysical Surveys Raw Data File 2025-13, 6 p. https://doi.org/10.14509/31537

Moshrefzadeh, J.A., Naibert, T.J., Hofmann, Florian, Newberry, R.J., Twelker, Evan, and Buchanan, J.W., 2026, $^{40}Ar/^{39}Ar$ geochronology data from the Big Delta and Circle quadrangles, Alaska: Alaska Division of Geological & Geophysical Surveys Raw Data File 2026-14, 55 p. https://doi.org/10.14509/32086

Naibert, T.J., Benowitz, J.A., Wypych, Alicja, Sicard, K.R., and Twelker, Evan, 2020, $^{40}Ar/^{39}Ar$ data from the Tanacross D-1 and parts of the D-2, C-1, and C-2 quadrangles, Alaska: Alaska Division of Geological & Geophysical Surveys Raw Data File 2020-12, 35 p. https://doi.org/10.14509/30466

Naibert, T.J., Wypych, Alicja, Newberry, R.J., Twelker, Evan, Gavel, M.M., Wildland, A.D., Barrera, M.L., Szumigala, D.J., Regan, S.P., Avirett, D.F., Bernard, C.M., Blackwell, N.J., Fessenden, S.N., Harvey, D.A., Hubbard, A.K., Masterman, S.S., Muller, I.P., Turner, M.M., and Wyatt, W.C., 2024, Geologic background and map unit descriptions to accompany bedrock geologic maps of the western Tanacross and Taylor Mountain areas, Tanacross and Eagle quadrangles, Alaska: Alaska Division of Geological & Geophysical Surveys Preliminary Interpretive Report 2024-6A, 39 p. https://doi.org/10.14509/31167

Newberry, R.J., Bundtzen, T.K., Clautice, K.H., Combellick, R.A., Douglas, Tom, Laird, G.M., Liss, S.A., Pinney, D.S., Reifenstuhl, R.R., and Solie, D.N., 1996, Preliminary geologic map of the Fairbanks mining district, Alaska: Alaska Division of Geological & Geophysical Surveys Public Data File 96-16, 17 p., 2 sheets, scale 1:63,360. https://doi.org/10.14509/1740

Newberry, R.J., Bundtzen, T.K., Mortensen, J.K., and Weber, F.R., 1998, Petrology, geochemistry, age, and significance of two foliated intrusions in the Fairbanks District, Alaska: U.S. Geological Survey Professional Paper 1595, p. 117–129.

Newberry, R.J., and Twelker, Evan, 2021, Metamorphism of the Ladue River-Mount Fairplay area: Alaska Division of Geological & Geophysical Surveys Report of Investigation 2021-5B, p. 33–39. https://doi.org/10.14509/30736

Newberry, R.J., and Moshrefzadeh, J.A., 2026, Interior Alaska amphibolite mineral compositions: A key to distinguishing metamorphic assemblage: Alaska Division of Geological & Geophysical Surveys Preliminary Interpretive Report 2026-2, 33 p. https://doi.org/10.14509/32081

Pavlis, T.L., Sisson, V.B., Foster, H.L., Nokleberg, W.J., and Plafker, George, 1993, Mid-Cretaceous extensional tectonics of the Yukon-Tanana Terrane, Trans-Alaska Crustal Transect (TACT), east-central Alaska: Tectonics, v. 12, p. 103–122.

Pearce, Julian, and Cann, Johnson, 1973, Tectonic setting of basic volcanic rocks determined using trace element analyses: Earth and Planetary Science Letters, v. 19, p. 290–300. https://doi.org/10.1016/0012-821X(73)90129-5

Smith, T.E., Pessel, G.H., and Wiltse, M.A., eds., 1987, Mineral assessment of the Lime Peak-Mt. Prindle area, Alaska: Alaska Division of Geological & Geophysical Surveys Miscellaneous Publication 29, 712 p.

Smith, T.E., Pessel, G.H., and Wiltse, M.A., eds., 1987, Mineral assessment of the Lime Peak–Mt. Prindle area, Alaska: Alaska Division of Geological & Geophysical Surveys Miscellaneous Publication 29, 712 p., 13 sheets, scale 1:63,360. https://doi.org/10.14509/731

Smith, T.E., Robinson, M.S., Weber, F.R., Waythomas, C.F., and Reifenstuhl, R.R., 1994, Geologic map of the upper Chena River area, eastern interior Alaska: Alaska Division of Geological & Geophysical Surveys Professional Report 115, 19 p., 1 sheet, scale 1:63,360. https://doi.org/10.14509/2315

Smith, M.T., Thompson, J.F.H., Bressler, Jason, Layer, P.W., Mortensen, J.K., Abe, Ichiro, and Takaoka, Hidetoshi, 1999, Geology of the Liese Zone, Pogo Property, east-central Alaska: Society of Economic Geologists Newsletter, no. 38, p. 1–21.

Solie, D.N., Werdon, M.B., Freeman, L.K., Newberry, R.J., Szumigala, D.J., Speeter, G.G., and Elliott, B.A., 2019, Bedrock-geologic map, Alaska Highway corridor, Tetlin Junction, Alaska to Canada border: Alaska Division of Geological & Geophysical Surveys Preliminary Interpretive Report 2019-3, 16 p., 2 sheets, scale 1:63,360. https://doi.org/10.14509/30038

Southworth, D.D., 1984, Geologic and geochemical investigation of the Nail allochthon, east-central Alaska: U.S. Bureau of Mines Open-File Report 176-84, 21 p., 1 sheet, scale 1:250,000.

Todd, Erin, Kylander-Clark, Andrew, Kreiner, D.C., Jones, J.V. III, Holm-Denoma, C.S., and Wypych, Alicja, 2023, U-Pb ages, hafnium isotope ratios, and trace element concentrations by Laser-ablation Split Stream (LASS) analysis of igneous and metamorphic zircons from the Yukon–Tanana Upland, eastern Alaska: U.S. Geological Survey Data Release. https://doi.org/10.5066/P9O1DMIE

Twelker, Evan, Newberry, R.J., Naibert, T.J., Wypych, Alicja, Gavel, M.M., Barrera, M.L., Szumigala, D.J., Truskowski, C.M., Muller, I.P., Fessenden, S.N., Blackwell, N.J., Harvey, D.A., and Wildland, A.D., 2025, Bedrock geologic maps of the Mount Harper–Middle Fork area, Volkmar River–Healy River area, Goodpaster River–Shaw Creek area, and the Richardson Mining District, Alaska: Alaska Division of Geological & Geophysical Surveys Preliminary Interpretive Report 2025-2, 38 p. https://doi.org/10.14509/31648

Twelker, Evan, Newberry, R.J., Wypych, Alicja, Naibert, T.J., Wildland, A.D., Sicard, K.R., Regan, S.P., Athey, J.E., Wyatt, W.C., and Lopez, J.A., 2021, Bedrock geologic map of the Ladue River–Mount Fairplay area, Tanacross and Nabesna quadrangles, Alaska, in Twelker, Evan, ed., Geologic investigation of the Ladue River–Mount Fairplay area, eastern Alaska: Alaska Division of Geological & Geophysical Surveys Report of Investigation 2021-5A, p. 1–32, 1 sheet, scale 1:100,000. https://doi.org/10.14509/30735

Weber, F.R., Foster, H.L., Keith, T.E.C., and Dusel-Bacon, Cynthia, 1978, Preliminary geologic map of the Big Delta Quadrangle, Alaska: U.S. Geological Survey Open-File Report 78-529-A, 1 sheet, scale 1:250,000.

Werdon, M.B., Athey, J.E., Szumigala, D.J., Newberry, R.J., Grady, J.C., and Munly, W.C., 2001, Major-oxide, minor-oxide, trace-element, and geochemical data from rocks collected in the Salcha River–Pogo area in 2000, Big Delta and northwestern Eagle quadrangles, Alaska: Alaska Division of Geological & Geophysical Surveys Raw Data File 2001-1, 19 p., 1 sheet, scale 1:250,000. https://doi.org/10.14509/2661

Werdon, M.B., Newberry, R.J., Athey, J.E., and Szumigala, D.J., 2004, Bedrock geologic map of the Salcha River–Pogo area, Big Delta Quadrangle, Alaska: Alaska Division of Geological & Geophysical Surveys Report of Investigation 2004-1B, 19 p., 1 sheet, scale 1:63,360. https://doi.org/10.14509/3209

Werdon, M.B., Newberry, R.J., Athey, J.E., Szumigala, D.J., Freeman, L.K., Lessard, R.R., Hendry, K.R., and Wiltse, M.A., 2003, Major-oxide, minor-oxide, trace-element, and geochemical data from rocks collected in the Big Delta Quadrangle, Alaska in 2002: Alaska Division of Geological & Geophysical Surveys Raw Data File 2003-2, 45 p. https://doi.org/10.14509/2997

Wildland, A.D., 2022, Temporal links between ductile shearing, widespread plutonism, and tectonic exhumation near the boundary of parautochthonous and allochthonous terranes in the northern Cordillera, Alaska: University of Alaska Fairbanks, M.S. thesis, 67 p.

Wiltse, M.A., Reger, R.D., Newberry, R.J., Pessel, G.H., Pinney, D.S., Robinson, M.S., and Solie, D.N., 1995, Bedrock geologic map of the Circle mining district, Alaska: Alaska Division of Geological & Geophysical Surveys Report of Investigation 95-2B, 1 sheet, scale 1:63,360. https://doi.org/10.14509/2515

Wilson, F.H., Hults, C.P., Mull, C.G., and Karl, S.M., 2015, Geologic map of Alaska: U.S. Geological Survey Scientific Investigations Map 3340, 196 p., 2 sheets, scale 1:1,584,000. https://alaska.usgs.gov/science/geology/state_map/interactive_map/AKgeologic_map.html

Wypych, Alicja, Hubbard, T.D., Naibert, T.J., Athey, J.E., Newberry, R.J., Sicard, K.R., Twelker, Evan, Werdon, M.B., Willingham, A.L., Wyatt, W.C., and Lockett, A.C., 2021, Northeast Tanacross geologic map and map units and descriptions, in Wypych, Alicja, ed., Northeast Tanacross geologic mapping project, Alaska: Alaska Division of Geological & Geophysical Surveys Report of Investigation 2020-9B, p. 9–26, 1 sheet, scale 1:63,360. https://doi.org/10.14509/30539

Wypych, Alicja, Jones, J.V. III, and O'Sullivan, Paul, 2020, U-Pb zircon ages from bedrock samples collected in the Tanacross D-1 and parts of the D-2, C-1, and C-2 quadrangles, Alaska: Alaska Division of Geological & Geophysical Surveys Preliminary Interpretive Report 2020-2, 19 p. https://doi.org/10.14509/30465

Yukon Geological Survey, 2019, Yukon bedrock geology map: Yukon Geological Survey webmap, accessed March 19, 2019, https://yukon.ca/en/yukon-geology#bedrock-geology

APPENDIX

Table A-1. U-Pb zircon ages generated as part of this project. See referenced data releases for additional information.

Sample ID	Map Unit	Age (Ma)	2 Sigma Age Error (Ma)	Latitude	Longitude	Reference
23ADW001	PEm	56.51	0.37	65.080301	-145.787388	Buchanan, Barrera, and others, 2025
24MLB243	PEfp	56.67	0.93	65.460397	-144.616485	Buchanan, Barrera, and others, 2025
23TJN040	PEfp	57.32	0.37	65.073435	-145.772513	Buchanan, Barrera, and others, 2025
23ET064	PEfp	57.89	0.46	64.645200	-144.204000	Buchanan, Gavel, Barerra and others, 2025
23ET223	PEfp	59.86	0.26	64.826806	-146.197691	Buchanan, Barrera, and others, 2025
23TJN064	lKeg	66.70	1.20	64.888034	-146.165657	Buchanan, Barrera, and others, 2025
24CMT102	lKeg	67.50	0.71	65.178447	-144.559039	Buchanan, Barrera, and others, 2025
23IPM132	lKeg	67.82	0.92	64.876366	-146.182778	Buchanan, Gavel, Barerra, and others, 2025
23JWB145	lKeg	69.20	0.43	65.120197	-144.934399	Buchanan, Barrera, and others, 2025
24Z312	lKeg	69.93	0.36	65.123906	-144.716467	Buchanan, Barrera, and others, 2025
23Z388	lKeg	70.68	0.41	65.080945	-146.067554	Buchanan, Barrera, and others, 2025
23MLB206	lKeg	70.75	0.96	64.676228	-146.754309	Buchanan, Gavel, Barerra, and others, 2025
23Z467	lKeg	71.62	0.32	64.726575	-147.193159	Buchanan, Barrera, and others, 2025
23RN540	lKeg	71.80	0.33	64.732800	-146.747400	Buchanan, Gavel, Barerra, and others, 2025
24MLB181	lKeg	71.98	0.88	65.113444	-144.083389	Buchanan, Barrera, and others, 2025
23RN276	lKeg	72.38	0.35	64.854597	-146.271719	Buchanan, Barrera, and others, 2025
24Z315	lKeg	76.51	0.39	65.162064	-144.650643	Buchanan, Barrera, and others, 2025
23JNB024	Kfsg	90.10	0.90	65.086894	-145.107849	Buchanan, Gavel, Barerra, and others, 2025
24Z014	Kfsgd	90.41	0.44	65.004077	-144.628666	Buchanan, Barrera, and others, 2025
24JWB095	Kfsg	91.13	0.62	65.305110	-144.200541	Buchanan, Barrera, and others, 2025
24RN358	Kfsg	91.39	0.53	65.195654	-144.505454	Buchanan, Barrera, and others, 2025
23RN166	Kfsg	91.46	0.59	64.908300	-146.167100	Buchanan, Gavel, Barerra, and others, 2025

Sample ID	Map Unit	Age (Ma)	2 Sigma Age Error (Ma)	Latitude	Longitude	Reference
23RN386	Kfsg	91.60	1.50	65.044000	-146.036800	Buchanan, Gavel, Barerra, and others, 2025
23RN183	Kfsqd	92.83	0.72	64.937100	-146.233300	Buchanan, Gavel, Barerra, and others, 2025
23IPM200	Kfsg	93.01	0.52	65.026300	-146.191800	Buchanan, Gavel, Barerra, and others, 2025
23RN618	Kfsg	93.48	0.41	64.903766	-146.367231	Buchanan, Barrera, and others, 2025
23Z330	Kfsg	94.26	0.57	64.826567	-144.870964	Buchanan, Gavel, Barerra, and others, 2025
23TJN092	Kfsgd	94.30	0.43	64.724542	-144.550936	Buchanan, Barrera, and others, 2025
24ET128	Kfsgd	94.63	0.55	65.282590	-144.297407	Buchanan, Barrera, and others, 2025
23RN248	Kfsg	95.20	1.20	64.893800	-145.719100	Buchanan, Gavel, Barerra, and others, 2025
23Z150	Kfsg	95.67	0.44	64.612726	-144.773191	Buchanan, Gavel, Barerra, and others, 2025
23Z331	Kfsg	96.20	0.52	64.736871	-145.384478	Buchanan, Barrera, and others, 2025
24MLB029	Kfst	96.50	0.49	64.859636	-144.119085	Buchanan, Barrera, and others, 2025
23RN487	Kfsmg	97.40	0.78	65.071923	-145.935966	Buchanan, Barrera, and others, 2025
24Z044	Kfsgd	97.53	0.61	65.001453	-144.460430	Buchanan, Barrera, and others, 2025
24JWB051	Kfsgd	98.14	0.38	64.903579	-144.126636	Buchanan, Barrera, and others, 2025
24ET154	Kfsqd	100.55	0.64	64.896815	-146.810508	Buchanan, Barrera, and others, 2025
24Z054	Khg	105.95	0.63	64.743201	-144.143430	Buchanan, Barrera, and others, 2025
23ET060	Khgd	108.17	0.77	64.467300	-144.526400	Buchanan, Gavel, Barerra, and others, 2025
23MLB111	Khmg	108.30	1.60	64.589600	-145.746200	Buchanan, Gavel, Barerra, and others, 2025
23RN083	Khgd	110.25	0.89	64.505600	-144.228800	Buchanan, Gavel, Barerra, and others, 2025
23MMG150	Khg	110.70	1.10	65.062848	-144.597387	Buchanan, Gavel, Barerra, and others, 2025
23IPM068	Khg	111.30	1.70	64.528253	-144.649073	Buchanan, Gavel, Barerra, and others, 2025
23MMG038	Khgd	112.10	1.10	64.453978	-145.062559	Buchanan, Gavel, Barerra, and others, 2025
24TJN055	MDlo	113.50	1.00	64.863834	-144.088611	Buchanan, Barrera, and others, 2025
76AWr287	MDbf	361.10	2.50	64.831839	-145.590568	Buchanan, Barrera, and Newberry, 2026

Sample ID	Map Unit	Age (Ma)	2 Sigma Age Error (Ma)	Latitude	Longitude	Reference
23JWB090	pMblf	361.30	2.00	64.875465	-146.045817	Buchanan, Barrera, and others, 2025
23RN513	MDbf	365.30	2.10	64.631259	-146.642194	Buchanan, Barrera, and others, 2025
23JWB125	Omum	481.80	1.40	64.893422	-145.396257	Buchanan, Barrera, and others, 2025

Table A-2. Statistical summary of magnetic susceptibility by map unit. Geologists collected 1–12 measurements at each field station using handheld KT-10 magnetic susceptibility meters. This table reflects the values for stations within polygons of a given unit, as mapped.

Rock unit	Mean	Minimum	25th Percentile	50th Percentile	75th Percentile	Maximum	n (stations)	n (measurements)
Sedimentary rocks								
CzKs	0.04	0.01	0.03	0.04	0.04	0.1	5	29
Volcanic rocks								
ⱣEr	4.66	3.8	3.94	4.62	5.17	6.03	1	8
Slate Creek intrusive suite								
ⱣEm	1.29	0.15	0.62	0.74	1.77	3.2	14	132
ⱣEfp	0.21	0.01	0.07	0.09	0.22	0.86	23	189
Eielson plutonic suite								
lKeg	0.14	0.01	0.04	0.06	0.08	2.96	121	1193
Taurus plutonic suite								
lKpg	1.28	0.06	0.3	0.74	1.18	6.03	9	56
Fairbanks-Salcha plutonic suite								
Kfsg	0.11	0.01	0.06	0.09	0.14	0.63	291	2361
Kfsgd	0.34	0.02	0.09	0.14	0.19	8.46	119	842
Kfsmg	0.09	0.01	0.05	0.06	0.08	0.76	37	355
Kfsp	0.4	0	0.05	0.07	0.12	1.75	5	43
Kfsqd	0.62	0.07	0.17	0.26	0.35	7.35	63	216
Kfst	0.24	0.1	0.16	0.25	0.27	0.67	17	163
Harper plutonic suite								
Khg	0.22	0.01	0.08	0.11	0.13	3.71	141	797
Khgd	0.53	0.02	0.09	0.13	0.18	12.3	241	929
Khmg	0.11	0.01	0.02	0.04	0.15	0.7	14	28

Rock unit	Mean	Minimum	25th Percentile	50th Percentile	75th Percentile	Maximum	n (stations)	n (measurements)
Khdi*								
Other intrusive rocks								
Kmi	0.51	0.14	0.34	0.4	0.52	1.44	8	29
KPzi	0.13	0.07	0.1	0.11	0.15	0.25	12	55
Seventymile terrane								
TRMsmg	1.15	0	0.15	0.25	0.39	20.9	46	340
TRMscg	1.68	0	0.04	0.13	0.24	22.8	21	183
TRMsmm	2.8	0.02	0.24	0.41	0.67	50.2	170	1075
TRMsmu	13.9	0.07	3.42	11.04	20.38	62.75	115	883
Butte assemblage								
MDbf	0.11	0.03	0.06	0.08	0.12	0.32	52	358
MDbm	0.44	0.01	0.05	0.07	0.25	18	68	546
MDbmc	0.1	0.02	0.06	0.09	0.12	0.31	58	535
MDbmg	0.12	0	0.06	0.09	0.16	0.49	221	1573
MDbmm	3.93	0.03	0.17	0.39	0.6	139.5	304	2254
MDbms	0.69	0	0.08	0.12	0.2	227.75	917	4795
Blackshell assemblage								
pMbl	0.23	0	0.03	0.06	0.12	34.05	433	3750
pMblc	0.24	0.01	0.07	0.14	0.21	5.35	167	1609
pMblf	0.09	0.02	0.06	0.08	0.12	0.17	9	65
pMblq	0.14	0.02	0.04	0.09	0.19	0.45	20	185
Ordovician mafic and ultramafic rocks								
Omum	35.07	0.58	17.82	35.07	52.31	69.55	2	22

Rock unit	Mean	Minimum	25th Percentile	50th Percentile	75th Percentile	Maximum	n (stations)	n (measurements)
Preacher assemblage								
PzPpcm	0.11	0	0.05	0.06	0.12	0.46	12	102
PzPpcp	0.12	0.1	0.11	0.12	0.14	0.15	2	18
PzPpmm	0.44	0.44	0.44	0.44	0.44	0.44	1	12
PzPpsg	0.09	0.01	0.05	0.07	0.11	0.29	87	727
PzPpsp	0.15	0.03	0.08	0.14	0.2	0.4	19	134
Fairbanks-Chena assemblage								
TrPzfcu	18.09	0.12	0.56	9.52	26.48	82.7	68	366
MDcag	0.18	0	0.09	0.11	0.15	3.31	184	1223
MDfca	1.46	0	0.17	0.36	0.56	56.3	529	2431
MDfco	0.35	0	0.07	0.1	0.15	38.3	550	2062
pMfccs	0.3	0.12	0.17	0.24	0.3	0.79	10	90
pMfcg	0.06	0.01	0.02	0.03	0.09	0.16	3	17
pMfcm	0.08	0.01	0.03	0.08	0.1	0.21	15	134
pMfcp	0.26	0.03	0.07	0.1	0.15	11.1	76	706
pMfcq	0.1	0	0.04	0.08	0.14	0.4	173	623
pMfcqp	0.09	0.02	0.04	0.07	0.12	0.2	28	281
pMfcrg	0.13	0.01	0.07	0.11	0.16	1.65	383	1289
pMfcs	0.18	0.02	0.11	0.18	0.24	0.59	71	639
pMfcsc	0.19	0.02	0.12	0.18	0.23	0.67	102	914
pMfcsg	0.22	0	0.09	0.14	0.21	27.3	1346	10343
Lake George assemblage								
MDla	0.79	0.4	0.54	0.61	0.79	1.84	8	79

Rock unit	Mean	Minimum	25th Percentile	50th Percentile	75th Percentile	Maximum	n (stations)	n (measurements)
MDlo	0.13	0.02	0.07	0.1	0.15	2.03	212	745
pMlmpg	0.13	0.02	0.08	0.14	0.18	0.25	27	233
pMlms	0.28	0.04	0.12	0.18	0.26	2.29	64	403
pMlp	0.31	0.01	0.03	0.12	0.17	7.37	38	320
pMlrp	0.13	0	0.08	0.12	0.17	0.7	414	2257

* unit compiled from Day and others (2007) and not resampled by DGGS